Molecular Plant
Research article

CellPress
Partner Journal

Plant triterpenoid saponins function as susceptibility factors to promote the pathogenicity of *Botrytis cinerea*

Francisco J. Escaray, Amelia Felipo-Benavent, Cristian J. Antonelli, Begoña Balaguer, Maria Pilar Lopez-Gresa and Pablo Vera*

Instituto de Biología Molecular y Celular de Plantas, Universidad Politécnica de Valencia-C.S.I.C, Ciudad Politécnica de la Innovación, Edificio 8E, acceso G, Ingeniero Fausto Elio, s/n, 46022 Valencia, Spain

***Correspondence: Pablo Vera (vera@ibmcp.upv.es)**

https://doi.org/10.1016/j.molp.2024.05.008

ABSTRACT

The gray mold fungus *Botrytis cinerea* is a necrotrophic pathogen that causes diseases in hundreds of plant species, including high-value crops. Its polyxenous nature and pathogenic success are due to its ability to perceive host signals in its favor. In this study, we found that laticifer cells of *Euphorbia lathyris* are a source of susceptibility factors required by *B. cinerea* to cause disease. Consequently, poor-in-latex (*pil*) mutants, which lack laticifer cells, show full resistance to this pathogen, whereas *lot-of-latex* mutants, which produce more laticifer cells, are hypersusceptible. These S factors are triterpenoid saponins, which are widely distributed natural products of vast structural diversity. The downregulation of laticifer-specific *oxydosqualene cyclase* genes, which encode the first committed step enzymes for triterpene and, therefore, saponin biosynthesis, conferred disease resistance to *B. cinerea*. Likewise, the *Medicago truncatula lha-1* mutant, compromised in triterpenoid saponin biosynthesis, showed enhanced resistance. Interestingly, the application of different purified triterpenoid saponins pharmacologically complemented the disease-resistant phenotype of *pil* and *hla-1* mutants and enhanced disease susceptibility in different plant species. We found that triterpenoid saponins function as plant cues that signal transcriptional reprogramming in *B. cinerea*, leading to a change in its growth habit and infection strategy, culminating in the abundant formation of infection cushions, the multicellular appressoria apparatus dedicated to plant penetration and biomass destruction in *B. cinerea*. Taken together, these results provide an explanation for how plant triterpenoid saponins function as disease susceptibility factors to promote *B. cinerea* pathogenicity.

Key words: *Euphorbia lathyris*, laticifer cell, latex, appressorium, infection cushion, necrotrophic fungi

Escaray F.J., Felipo-Benavent A., Antonelli C.J., Balaguer B., Lopez-Gresa M.P., and Vera P. (2024). Plant triterpenoid saponins function as susceptibility factors to promote the pathogenicity of *Botrytis cinerea*. Mol. Plant. **17**, 1073–1089.

INTRODUCTION

Plants inhabit natural environments rich in pathogens, which permanently threaten plant survival. However, not all pathogens are capable of successfully colonizing a specific host, which indicates the existence of efficient recognition mechanisms that lead to disease in susceptible hosts. Pathogen perception by the host is mediated via plant pattern recognition receptors (PRRs), which recognize pathogen-associated molecular patterns and plant-generated molecules known as damage-associated molecular patterns derived from the affected tissue upon initial infection. PRR-mediated signaling is an efficient form of pathogen monitoring in plants that triggers defense responses known as pattern-triggered immunity (PTI), which provides protection against diseases (Yuan et al., 2021). The fungal necrotroph *Botrytis cinerea*, which causes gray mold disease, is a generalist pathogen that infects a wide range of plant species, including important agricultural crops (Van Kan, 2006; Dean et al., 2012; Mengiste, 2012; Fillinger and Elad, 2015). The fungal cell wall component chitin and secreted plant cell wall-degrading enzymes (PCWDEs), including polygalacturonase, are characteristic *B. cinerea* pathogen-associated molecular patterns (Poinssot et al., 2003; Bi et al., 2022). Upon initial infection, polygalacturonase degrades plant cell wall pectin

Published by the Molecular Plant Shanghai Editorial Office in association with Cell Press, an imprint of Elsevier Inc., on behalf of CSPB and CEMPS, CAS.

(the primary carbon source for the pathogen) and releases oligogalacturonides, which function as damage-associated molecular patterns to activate defense responses. From a disease dynamics perspective, there is an early infection stage that leads to the killing of a discrete number of plant cells, in which fungal biomass starts accumulating. This stage of infection is mediated by the formation, soon after conidia germination, of a chitin-enriched unicellular appressorium (UA), which is in charge of secretion of PCWDEs and deployment of toxins, cell-death-inducing proteins (CDIPs), and compounds promoting regulated cell death. This results in the formation of an infection court that leads to the initiation of a secondary and more aggressive phase of fungal growth, resulting in the emergence of visible necrosis in the plant (Bi et al., 2022). Plants respond to this initial phase of infection with timely regulation of immune responses, which involves the coordinated action of hormones, such as jasmonic acid (Lorenzo et al., 2004) and abscisic acid (García-Andrade et al., 2020), that coordinate the reprogramming of the plant defense machinery to counteract *B. cinerea*. In addition, secondary metabolites, including phytoalexin camalexin (Bednarek et al., 2009) and dynamic remodeling of the plant extracellular matrix (Ellis et al., 2002; Cantu et al., 2008; Ramírez et al., 2011a, 2011b), together with other biochemical processes, including callose deposition (Wang et al., 2021a), plastidial mRNA editing control mediated by the OCP3 factor (Coego et al., 2005; García-Andrade et al., 2013), and epigenetic control (López et al., 2011), are also critical components that contribute to the degree of disease caused by *B. cinerea*. Since the toolbox of *B. cinerea* does not include host-specific Avr effectors, and no single gene confers plant resistance against the fungus, effector-triggered immunity (ETI) does not seem to be operative, which indicates that resistance to *B. cinerea* is quantitative rather than complete (Corwin and Kliebenstein, 2017). In the absence of ETI, the virulence of *B. cinerea* appears proportional to the degree of PTI activation, where the BOTRYTIS INDUCED KINASE (BIK1) plays a pivotal role by integrating PTI signals downstream of multiple PRRs (Laluk et al., 2011), which subsequently leads to the production of defense compounds aimed at limiting local infection (Veronese et al., 2006; Ahuja et al., 2012).

Most pathogens, along with evasion of plant immunity, require the identification of host constituents to establish compatible interactions. Plant factors that facilitate infection and support compatibility are considered susceptibility (S) factors encoded by *S* genes (Van Schie and Takken, 2014). Mutation or loss of an *S* gene can therefore limit the ability of the pathogen to cause disease, either because of impaired pre-penetration requirements, such as host recognition, or impaired support of specific post-penetration requirements, such as the availability of nutrients. One of the best-known *S* genes is the *mildew resistance locus O* (*MLO*), required for powdery mildew penetration of epidermal cells in a wide variety of plant species (Bü and Hollricher, 1997). MLO appears to be required for susceptibility to adapted pathogens, and *mlo* mutants display a loss of susceptibility (Humphry et al., 2006). Likewise, components of the plant cuticle mediate susceptibility (Bessire et al., 2007), and the genes that encode their biosynthetic enzymes are considered *S* genes. Similarly, expansin EXLA2, which mediates plant cell wall stretching and growth, is another S factor that mediates susceptibility to *B. cinerea* (Abuqamar et al., 2013). Despite this knowledge, identification of plant disease susceptibility factors that aid *B. cinerea* in gaining access to host plant cells remains limited.

Here, through the characterization of a previously identified disease-promoting activity toward *B. cinerea* synthesized in the laticifer cells of *E. lathyris*, we have identified that triterpenoid saponins (i.e., glycosylated triterpenes derived from 2,3-oxidosqualene upon its cyclation by oxidosqualene cyclase [OSC] enzymes) appear as plant factors essential to promote disease susceptibility to *B. cinerea*. Analysis of *OSC*-silenced plants and of stable mutant plants compromised in the synthesis of triterpenoid saponins confirmed the importance of these plant metabolites in mediating susceptibility to this pathogen. We further investigated the effect of saponins on *B. cinerea* and found that these secondary metabolites promote fungal transcriptional reprogramming, leading to a shift in the aggressive mode of growth of the pathogen, which promotes hypervirulence owing to the development of abundant multicellular appressoria known as infection cushions (ICs), which are considered fungal weapons of plant tissue destruction. Our study provides insights into the emergence of saponins as new S factors for *B. cinerea* infection and opens new avenues for engineering resistance to this fungus in crops.

RESULTS

E. lathyris latex is enriched in compounds promoting *B. cinerea* growth

Previously, we identified that latex produced in laticifer cells of *E. lathyris* plants was a source of *B. cinerea* conidia germination-promoting activity that fostered disease susceptibility (Castelblanque et al., 2021). Preliminary characterization studies revealed that it was a low-molecular-weight (ca. 1.3 kDa) polar compound. We hypothesized that such compound(s) might function as plant cues, which, upon being sensed by the pathogen, might signal its virulence. Aiming to identify the nature of the compound, an activity-guided fractionation from latex was performed employing a tandem FPLC ion exchange chromatography through SP- and Q-Sepharose followed by size exclusion chromatography (SEC) through Superdex 75 10/300 column (see section "materials and methods"). A final FPLC purification step using an SEC Superdex 30 column allowed the recovery of a peak of maximum activity promoting the *in vitro* germination of *B. cinerea* conidia (SEC 28–30 fractions; Figure 1A). Further partitioning of the SEC28–30 constituents by high-pressure liquid chromatography (HPLC) using an MeOH elution gradient (Figure 1B) showed that the activity eluted between 14 and 17 min (fraction iii), corresponding to 75%–82% of MeOH. Mass spectrometry (MS) indicated this fraction contained four major compounds eluting at 14.97, 15.51, 15.98, and 16.51 min, which corresponded to 1118.4, 1130.5, 1130.4, and 1114.4 *m/z*, respectively (Figure 1C). Metlin database search (Smith et al., 2005) commonly matched the four *m/z* values to three different plant triterpenoid-derived saponins: achyranthoside D, α-aescin, and lycoperoside A. Therefore, we hypothesized that distinct saponins (i.e., glycosides of triterpenes) produced in the laticifer cells of

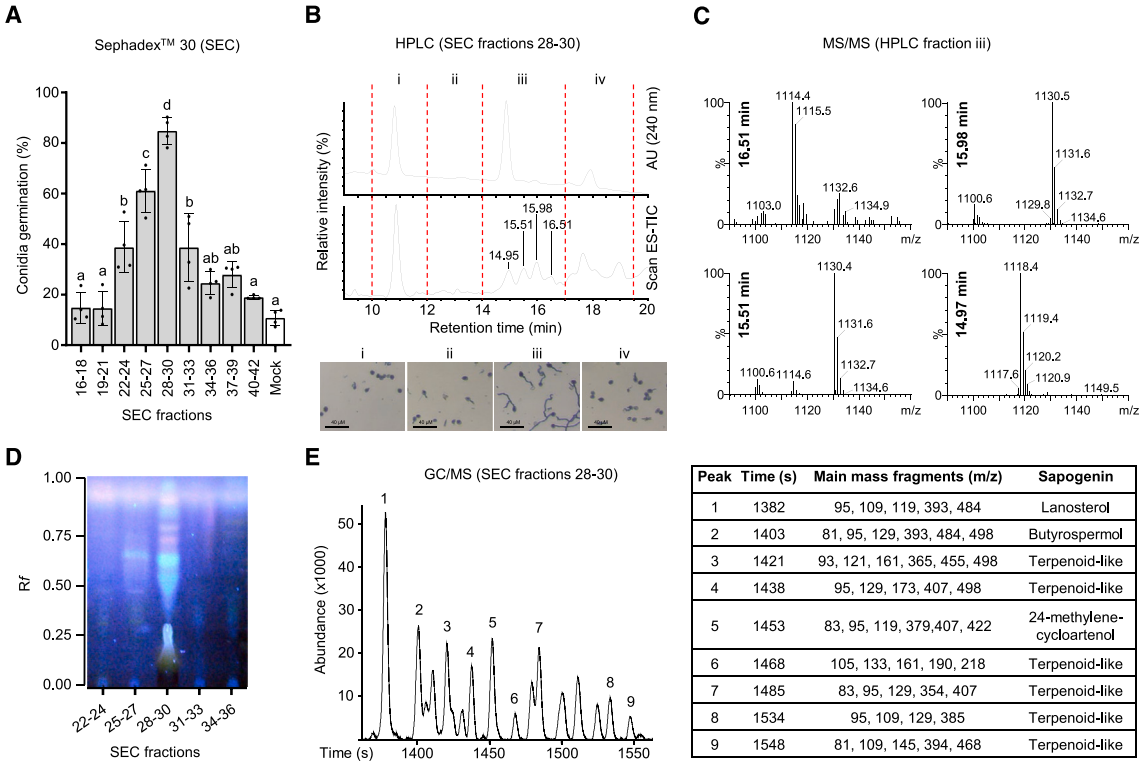

Peak	Time (s)	Main mass fragments (m/z)	Sapogenin
1	1382	95, 109, 119, 393, 484	Lanosterol
2	1403	81, 95, 129, 393, 484, 498	Butyrospermol
3	1421	93, 121, 161, 365, 455, 498	Terpenoid-like
4	1438	95, 129, 173, 407, 498	Terpenoid-like
5	1453	83, 95, 119, 379,407, 422	24-methylene-cycloartenol
6	1468	105, 133, 161, 190, 218	Terpenoid-like
7	1485	83, 95, 129, 354, 407	Terpenoid-like
8	1534	95, 109, 129, 385	Terpenoid-like
9	1548	81, 109, 145, 394, 468	Terpenoid-like

Figure 1. Purification of conidial germination-promoting activity present in the latex of *E. lathyris* plants.

(A) *B. cinerea* conidial germination assay of the eluted fractions from a Sephadex 30 column used to fractionate latex constituents by size exclusion chromatography (SEC). SEC fractions 28–30 showed the highest activity for promoting conidial germination. Bars indicate the mean ± SEM obtained from four biological replicates, and letters indicate significant differences ($p < 0.05$; ANOVA test, Bonferroni's test).

(B) HPLC fractionation of the pooled SEC28–30 fractions in a C18 reverse-phase column and elution with a 55%–100% methanol linear gradient. The chromatograms were recorded using either continuous PDA scanning (upper) or negative ion mode electrospray ionization (ESI−, lower) intensities. Four peaks with different retention times were detected in fraction (iii), which showed the conidial germination activity. Pictures below the chromatograms show representative images of a conidia germination assay after incubation for 24 h with each of the four indicated HPLC fractions (i–iv). The conidia were stained with trypan blue.

(C) Mass spectra of the four individual peaks present in the HPLC fraction (iii) shown in **(B)**.

(D) TLC silica gel 60 of the SEC28–30 collected fractions shown in **(A)** upon staining with the Lieberman–Burchard reagent and visualization at 365 nm. The blue and red spots correspond to saponins.

(E) GC/MS analysis of the SEC28–30 fraction after HCl hydrolysis and subsequent extraction with heptane to reveal the presence of sapogenins. The chromatogram on the left shows the presence of different apolar molecules, of which nine corresponded to sapogenins upon MS/time-of-flight analysis and whose main mass fragments matched that of lanosterol (peak 1), butyrospermol (peak 2), and other terpenoid-like sapogenins.

E. lathyris might be responsible for the observed fungal growth-promoting activity. In fact, the SEC28–30 fraction showed a persisting foam upon agitation, which is characteristic of saponin-enriched extracts (Góral and Wojciechowski, 2020). Furthermore, separation of the SEC28–30 fraction by thin layer chromatography (TLC; silica gel 60), followed by staining with the Liebermann-Burchard reagent, which is specific for long-chain hydrocarbons and is used for saponin and sapogenin detection (Van Atta and Guggolz, 1958; Stochmal et al., 2008), revealed the presence of different saponin-like molecules with different *Rf* values (Figure 1D). Moreover, HCl hydrolysis of the saponin-enriched fraction, breaking the *O*-glycosidic and ester bonds present in the soluble glycosylated triterpenoids, and subsequent gas chromatography (GC)/MS analysis of the nonpolar fraction containing the aglycons of saponins (sapogenins) revealed up to nine peaks with different retention times (Figure 1E) and whose *m/z* values matched that of triterpenoid-like sapogenins, among which lanosterol and butyrospermol were the most abundant (Table in Figure 1E). The identified set of distinct saponins present in the latex of *E. lathyris* was named eulasaponins. Eight of these saponins were further purified by preparative TLC, and each individual saponin triggered the germination of water-suspended *B. cinerea* conidia and led to sustained germ tube elongation *in vitro* (Supplemental Figure 1). Therefore, these results point toward a generic non-collective role of eulasaponins in promoting *B. cinerea* germination and growth. The observed effect of the triterpenoid eulasaponins on conidial germination seems not to be related to a nutritional effect since addition of other chemical related metabolites at a similar concentration (50 μM), such as the alkaloid-based saponins Tomatin or Solanin, does not trigger germination of water-suspended *B. cinerea* conidia (Supplemental Figure 2). Interestingly, the addition of escin, which like eulasaponins is a triterpenoid-based saponin (see below), mirrored the eulasaponins' effect (Supplemental Figure 2), thus pointing toward triterpenoid saponins' specificity in promoting *B. cinerea* germination.

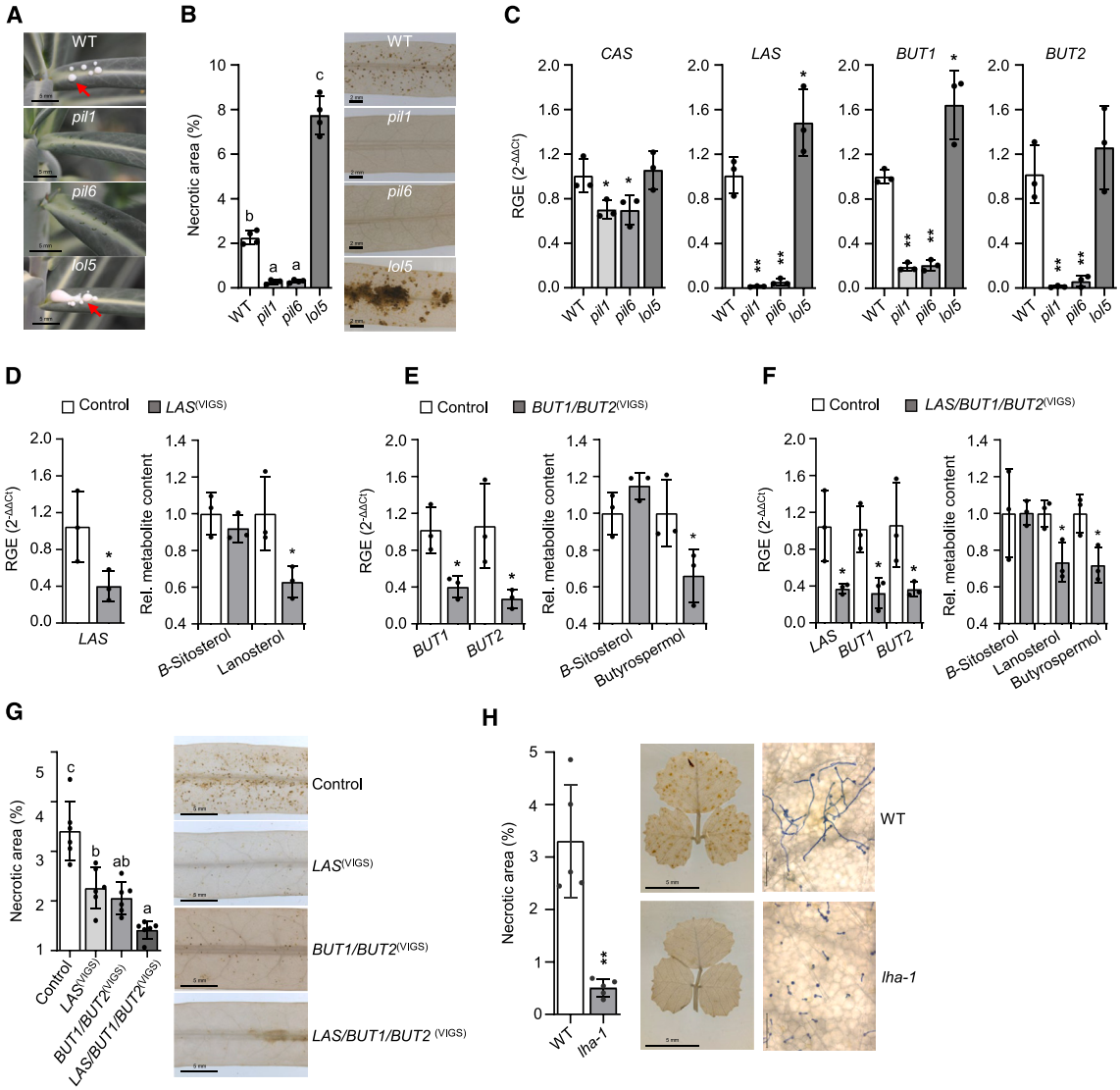

Figure 2. Silencing of *OSC* genes in *E. lathyris* reduces its susceptibility to *B. cinerea*.

(A) Latex-associated phenotypes of *poor-in-latex* (*pil*) and *lot-of-latex* (*lol5*) mutants compared to wild-type *E. lathyris* plants. Arrows indicate latex oozing upon pricking a leaf of wild-type and *lol5* plants, which is absent in *pil1* or *pil6* mutants.

(B) Enhanced disease resistance of the *pil1* and *pil6* mutants and enhanced disease susceptibility of *lol5* mutant, compared to wild-type plants, to *B. cinerea* infection. The necrotic area was recorded at 4 dpi with *B. cinerea*. Bars show the means ± SEM obtained from four biological replicates, and letters indicate significant differences (Brown–Forsythe and Welch ANOVA, Benjamini, Krieger and Yekutieli test, $p < 0.05$).

(C) Relative gene expression (RGE) of different *OSC* genes in wild-type, *pil1*, *pil6*, and *lol5* plants. *CAS*, cycloartenol synthase; *LAS*, lanosterol synthase; *BUT1* and *BUT2*, butyrospermol synthases. Bars show the means ± SEM obtained from three biological replicates; asterisks indicate significant differences compared to the wild type (*$p < 0.05$; **$p < 0.01$; pairwise fixed reallocation randomization test).

(D) Virus-induced gene silencing (VIGS) of *LAS* (*LAS*$^{(VIGS)}$ plants). Expression of the *LAS* gene (left) and accumulation of the triterpene lanosterol and β-sitosterol (right) in control and *LAS*$^{(VIGS)}$ plants are indicated. Bars show the means ± SEM obtained from three biological replicates; asterisks indicate significant differences compared to control plants ($p < 0.05$; Student's *t*-test).

(E) VIGS of *BUT1* and *BUT2* (*BUT1*/*BUT2*$^{(VIGS)}$ plants). Expression of *BUT1* and *BUT2* (left) and the accumulation of butyrospermol and β-sitosterol triterpenes (right) in control and *BUT1*/*BUT2*$^{(VIGS)}$ plants are indicated. Bars show the means ± SEM obtained from three biological replicates; asterisks indicate significant differences compared with control ($p < 0.05$; Student's *t*-test).

(F) VIGS of *LAS*, *BUT1*, and *BUT2* (*LAS*/*BUT1*/*BUT2*$^{(VIGS)}$ plants). *LAS*, *BUT1*, and *BUT2* gene expression (left) and accumulation of lanosterol, butyrospermol, and β-sitosterol (right), in *LAS*/*BUT1*/*BUT2*$^{(VIGS)}$ plants in comparison to control plants are indicated. Bars show the means ± SEM obtained from three biological replicates, asterisks indicate significant differences compared with the control expression level ($p < 0.05$; Student's *t*-test).

(G) Evaluation of disease caused by *B. cinerea* in *E. lathyris* *LAS*$^{(VIGS)}$, *BUT1*/*BUT2*$^{(VIGS)}$, and *LAS*/*BUT1*/*BUT2*$^{(VIGS)}$ plants in comparison to control (*MgCHL*$^{(VIGS)}$)plants. Bars show the means ± SEM obtained from six biological replicates, and letters indicate significant differences ($p < 0.05$; ANOVA test, Bonferroni's test).

(legend continued on next page)

Silencing of *OSC* genes in *E. lathyris* reduces its susceptibility to *B. cinerea*

Triterpenoids, the backbones of the identified eulasaponins, are synthesized by cyclization of the common precursor 2,3-oxydosqualene by specific OSCs, which represent the first committed step enzyme for saponin biosynthesis (Thimmappa et al., 2014). 2,3-Oxydosqualene is derived from squalene (by the action of squalene epoxidase), which is synthesized from isopentenyl pyrophosphate generated by the mevalonic acid pathway (Rohmer, 1999). In higher plants, OSC-mediated cyclation of 2,3-oxydosqualene marks the branch point between primary metabolism (e.g., phytosterols and cholesterol) and specialized secondary triterpene metabolism (Sawai and Saito, 2011).

Latex, along with the identified eulasaponins, is produced and accumulates in laticifer cells. Therefore, we hypothesized that laticifer cells might be a source of susceptibility to *B. cinerea.* In fact, *E. lathyris poor-in-latex* (*pil*) mutants (*pil1* and *pil6*) (Castelblanque et al., 2016), which are devoid of laticifer cells and produce no latex (Figure 2A), showed remarkable resistance to *B. cinerea* infection (Figure 2B and Castelblanque et al., 2021). Conversely, the *lot-of-latex 5* (*lol5*) mutant, which carries double the number of laticifer cells and produces more latex than wild-type plants (Castelblanque et al., 2018), developed susceptibility enhancement to *B. cinerea* (Figure 2B). The observed alteration in plant disease susceptibility correlated with a corresponding variation of fungal biomass growing on the inoculated plants (Supplemental Figure 3). Remarkably, *pil1*- and *pil6*-derived resistance concurs with compromised accumulation of triterpenoids (Castelblanque et al., 2016), whereas the *lol5*-derived enhanced susceptibility concurs with enhanced accumulation of triterpenoids (Castelblanque et al., 2018).

Based on these observations, we wondered which of the *OSCs* genes expressed in *E. lathyris* could be responsible for mediating the first-step biosynthesis of the sapogenin produced by laticifer cells. In plants, the *OSC* gene family has expanded to produce diverse triterpene scaffolds, with an average of 10–15 *OSC* genes per diploid genome (Thimmappa et al., 2014). A genome-mining approach enabled the identification of 15 *OSC* genes in the recently released *E. lathyris* genome (Wang et al., 2021b), which were clustered into four different groups: β-amyrin synthase-like, butyrospermol synthase-like (BUT), lanosterol synthase-like (LAS), and cycloartenol synthase-like (CAS) clusters (Supplemental Figure 4A). We then performed a comparative transcriptome analysis between wild-type and *pil1* plants, which revealed that three *OSC* genes (*Casp22865*, *Casp20664*, and *Casp30750*) were downregulated in *pil1* plants (fold change >2; $p < 0.05$; Supplemental Figure 4B). *Casp22865* and *Casp20664* (named *BUT1* and *BUT2*, respectively) encode proteins sharing 78% amino acid sequence identity homologous to butyrospermol cyclases (Supplemental Figure 4C). *Casp30750* (named *LAS1*) encodes the only lanosterol synthase homolog in *E. lathyris* (Supplemental Figure 4B). Furthermore, qRT-PCR analysis of wild-type, *pil1*, *pil6*, and *lol5* plants confirmed that *LAS*, *BUT1*, and *BUT2* were remarkably repressed in *pil1* and *pil6* plants but increased in the *lol5* mutant (Figure 2C), which is congruent with the compromised accumulation of free triterpenoids in the former mutants (Castelblanque et al., 2016) and their enhanced accumulation in the latter (Castelblanque et al., 2021). Analysis of *Casp30753* (*CAS*), which encodes cycloartenol synthase, used as a control in these experiments, showed no significant variation among the four genotypes. Therefore, *BUT1*, *BUT2*, and *LAS1* appeared to be laticifer-specific *OSC* genes.

Next, functional assays for the *OSC*s genes were performed. Since *E. lathyris* is recalcitrant to stable genetic transformation, we set up a protocol to generate knockdowns using tobacco rattle virus (TRV)-induced gene silencing (VIGS; Senthil-Kumar and Mysore, 2014; Aragonés et al., 2022) and *Agrobacterium* infiltration. First, we silenced a visible marker (magnesium chelatase subunit I [MgCHL]), which generates chlorosis when repressed. Supplemental Figure 5A shows that, when a 300-bp DNA sequence of the *E. lathyris MgCHL* gene was inserted into the TRV2 vector and agroinfiltrated into *E. lathyris* plants ($MgCHL^{(VIGS)}$), it rendered mosaic plants in which large sectors of the leaves were chlorotic, and this concurred with the downregulation of *MgCHL* recorded 10–14 days after agroinfiltration. Susceptibility to *B. cinerea* infection in $MgCHL^{(VIGS)}$ plants showed no significant variation when compared to non-agroinfiltrated plants (Supplemental Figure 5B). Subsequently, we attempted to silence *LAS1*, *BUT1*, and *BUT2* in combination with *MgCHL*, as the latter allows visual phenotyping for efficient silencing taking place. As *BUT1* and *BUT2* are highly homologous (Supplemental Figure 4C), a single DNA sequence was used to generate a single construct to downregulate both ($BUT1/BUT2^{(VIGS)}$). *LAS1*-derived VIGS construct, $LAS1^{(VIGS)}$, was designed to specifically downregulate this *OSC* gene. Upon agroinfiltration in combination with $MgCHL^{(VIGS)}$, only leaf samples with at least 40%–50% of the leaf surface showing chlorosis were sampled for subsequent analysis. In $LAS1^{(VIGS)}$ plants (Figure 2D), a significant reduction in *LAS1* gene expression was observed compared to control plants expressing only $MgCHL^{(VIGS)}$. GC/MS analysis of heptane extracts (Castelblanque et al., 2016) derived from the same leaf tissue samples, aimed at detecting the accumulation of lanosterol, showed a 40% reduction in $LAS1^{(VIGS)}$ plants compared with control plants (Figure 2D). In contrast, the accumulation of the triterpenoid β-sitosterol, used as an internal control, showed no variation (Figure 2D). Analysis of leaf samples derived from $BUT1/BUT2^{(VIGS)}$ plants revealed that both *BUT1* and *BUT2* gene expressions were strongly reduced, and this was mirrored by the reduced accumulation of the triterpenoid butyrospermol, but not of β-sitosterol (Figure 2E). The combined silencing of *LAS1*, *BUT1*, and *BUT2* genes was also examined in $LAS1/BUT1/BUT2^{(VIGS)}$ plants. This combination reduced the expression of these three genes and

(H) Disease caused by *B. cinerea* in *Medicago truncatula* wild-type plants is strongly reduced in *lha-1* plants. Bars show the means ± SEM obtained from five biological replicates; asterisks indicate significant difference compared with the control expression level (*t*-test with Welch's correction, $p = 0.003$). Comparative symptoms of the disease caused by *B. cinerea* in inoculated leaves are shown on the right. Conidial germination and hyphal development were strongly inhibited in the *lha-1* mutant compared to wild-type plants at 4 dpi, as revealed by trypan blue staining of the inoculated leaves.

significantly reduced both lanosterol and butyrospermol content (Figure 2F).

If eulasaponins function as disease susceptibility factors, then one would expect that a reduction in the triterpene scaffolds would render resistance enhancement to *B. cinerea*, thereby mimicking *pil* mutants (Figure 2B). Interestingly, when *LAS1*$^{(VIGS)}$ and *BUT1*/*BUT2*$^{(VIGS)}$ plants were assayed for susceptibility to *B. cinerea*, in comparison to control *MgCHL*$^{(VIGS)}$ plants, a significant resistance enhancement was recorded in both *OSCs*-silenced plants (Figure 2G). Furthermore, the enhanced resistance was even more pronounced in *LAS1*/*BUT1*/*BUT2*$^{(VIGS)}$ plants (Figure 2G), which presumably indicates additive effects. Therefore, maintaining intact lanosterol and butyrospermol biosynthesis, which are the major sapogenins accumulating in laticifer cells (Castelblanque et al., 2016), appears to be essential for *B. cinerea* to generate disease in *E. lathyris*.

The *Medicago truncatula lha-1* mutant, defective in triterpenoid saponins accumulation, is resistant to *B. cinerea*

Medicago is a plant genus showing major accumulation of triterpenoid saponins, which are mostly derived from the triterpene β-amyrin skeleton (Tava and Avato, 2006). Carelli et al. (2011) reported the first plant mutant in *M. truncatula*, named *lha-1*, compromised in triterpenoid saponins accumulation due to a loss of function in the *CYP716A12* gene, which is responsible for an early oxidative step of the β-amyrin skeleton previous to the addition of sugar moiety to the sapogenin. Therefore, if saponins are crucial for disease susceptibility to *B. cinerea*, then *lha-1* plants should exhibit altered susceptibility to this pathogen. Figure 2H illustrates that the high susceptibility of wild-type plants to *B. cinerea* was abrogated in *lha-1* plants, where disease symptoms were remarkably reduced (Figure 2H). The resistance of *lha-1* plants concurred with a reduction in *B. cinerea* conidia germination and a near absence of hyphal growth in the inoculated leaves (Figure 2H). Therefore, *lha*-1 enhanced resistance mirrors the phenotype of the *E. lathyris*-silenced plants (Figure 2G) and *pil1* and *pil6* mutants (Figure 2B). For the latter, conidial germination and hyphal growth are similarly impaired (Castelblanque et al., 2021). Thus, triterpenoid saponins also function in *M. truncatula* as host factors required by *B. cinerea* to promote disease.

External application of different saponins promoted *B. cinerea* growth and disease enhancement

We investigated saponins from other plant species. Escin is a triterpenoid saponin abundant in the seeds of horse chestnut plants (*Aesculum hippocastanum*), in which α- and β-aescin are predominant (Costantini, 1999). A highly purified commercially available preparation of escin (Supplemental Figure 1A) was assayed for *B. cinerea* growth-promoting activity. Under a range of different concentrations (30–120 μM) escin promoted nearly full germination of water-suspended conidia (Figure 3A), which was followed by elongation of the emerging hyphae. Avenacins are triterpenoid saponins found in the roots of oats (*Avena* spp.) and belong to a family of structurally related saponins (i.e., A-1/B-1/A-2/B-2) (Crombie et al., 1984). We purified avenacins from oat roots and isolated the most abundant A-1 isoform by using an LC-18 SPE column. In contrast to other saponins, avenacins fluoresce under ultraviolet illumination (Crombie et al., 1984), allowing for easy identification (Supplemental Figure 6A). Supplemental Figure 6B shows that avenacin A-1, under a range of concentrations (2.5–50 μM) also fully promoted conidial germination and sustained growth of the emerging hyphae. These observations further indicated that, irrespective of the plant source, different triterpenoid saponins exert a common effect on *B. cinerea*. This effect appears not to be specific to *B. cinerea*, since *Plectosphaerella cucumerina*, another fungal necrotroph, respond to the presence of escin with a similar germination enhancement (Supplemental Figure 7), which reconciles with previous observations (Castelblanque et al., 2021) that a latex-derived eulasaponin-enriched fraction also promoted *P. cucumerina* spore germination and enhanced disease susceptibility to this pathogen when exogenously applied to *Arabidopsis* plants.

The effects of the external application of the selected saponins was assessed *in planta*. When *E. lathyris* plants were spray inoculated with *B. cinerea* spores, disease susceptibility was enhanced if escin was applied at the time of inoculation, which translated into a significant increase in leaf surface area showing necrosis (Figure 3B). Moreover, the *B. cinerea*-resistant *pil1* and *pil6* plants, assayed in parallel, revealed that escin could override their characteristic resistance and gain back susceptibility (Figure 3B). The pharmacological complementation of *pil* mutants further supports the hypothesis that their strong resistance to *B. cinerea* is likely due to the lack of eulasaponins. Similarly, sprayed inoculation of *M. truncatula* plants with *B. cinerea* spores in the presence of escin also enhanced disease susceptibility (Figure 3C). Moreover, the *lha-1* resistant phenotype was abrogated by escin, and the mutant recovered a susceptibility that was similar to that of the wild-type plants (Figure 3C). Following the same rationale, we assayed the effect of escin on susceptibility in other plant species, including *Arabidopsis*, tomato, *Nicotiana benthamiana*, and rice (Figure 3D–3G). In all cases, the presence of escin promoted susceptibility enhancement to the fungus, which led to a notorious enlargement of the necrotic areas at the site of inoculation. In *A. thaliana* (Figure 3D), this escin-mediated susceptibility enhancement was remarkable, as it provoked complete maceration of the entire leaf by the fungi at 7 days post infection (dpi). The escin-mediated disease susceptibility enhancement to *B. cinerea* seems not to be the result of the saponin interfering with the plant immune response, since the induced expression of the *Arabidopsis PDF1.2* and *PR4* defense marker genes following escin treatment is not compromised (Supplemental Figure 8). Noteworthy was the result derived from rice plants, as, for this crop, there is lack of gray mold disease reported. Figure 3G shows the highly resistant phenotype of rice plants to *B. cinerea*, where infection hardly progressed. However, the presence of escin caused the fungus to extensively proliferate on the leaf surface, leading to infection, as observed at 4 dpi. Since grasses do not produce saponins (Osbourn, 2003), one is tempted to speculate that the lack of saponins might be on the basis that these plants are poor hosts for *B. cinerea*, and explains why the application of escin circumvents this condition in rice. Avenacin A, like escin, also promoted susceptibility enhancement, as exemplified in Supplemental

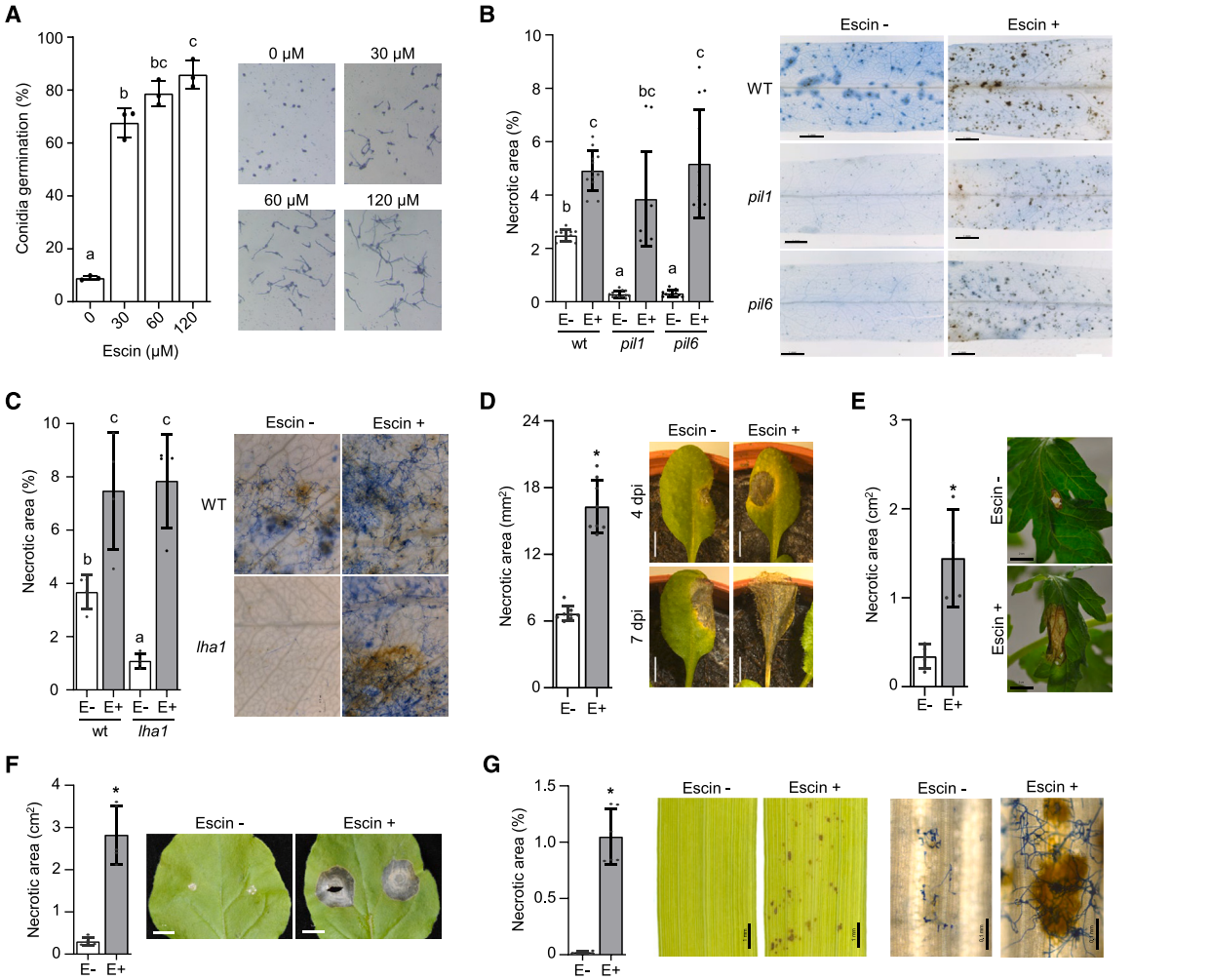

Figure 3. The external application of escin promotes susceptibility to *B. cinerea*.

(A) *In vitro* germination assay of *B. cinerea* conidia suspended in water and enhanced germination rate upon supplementation with different concentrations of escin. Bars show the mean ± SEM obtained from three biological replicates; different letters indicate significant differences ($p < 0.05$; ANOVA test, Bonferroni's test).

(B) Evaluation of disease symptoms, measured as the percentage of necrotic area, caused by *B. cinerea* at 4 dpi in *E. lathyris* wild-type, *pil1*, and *pil6* plants upon spray inoculation of spores in Gamborg medium in the presence (+) or absence (−) of escin (60 μM). Bars show the mean ± SEM obtained from 12 biological replicates; different letters indicate significant differences (Brown–Forsythe and Walch ANOVA test; Benjamini, Krieger, and Yekutieli test, $p < 0.05$).

(C) Disease susceptibility enhancement, recorded as percentage of the necrosis appearing in the inoculated leaves, caused by *B. cinerea* in *M. truncatula* wild-type and *lha-1* plants when inoculated by spraying in the presence (+) or absence (−) of escin (60 μM). Bars show the mean ± SEM obtained from four biological replicates; different letters indicate significant differences (Brown–Forsythe and Walch ANOVA test; Benjamini, Krieger, and Yekutieli test, $p < 0.05$). On the right, it is shown that the lack of hyphae growing in the inoculated leaves of *hla-1* plants is chemically complemented by the presence of escin.

(D–G) Escin-mediated disease susceptibility enhancement in different plant species. **(D)** *A. thaliana* Col-0 plants at 4 dpi (bars and pictures) and 7 dpi (pictures). Bars show the mean ± SEM obtained from eight biological replicates; asterisk indicates significant difference compared with the control (*t*-test with Welch's correction, $p < 0.0001$). **(E)** *Solanum lycopersicum* at 4 dpi. Bars show the mean ± SEM obtained from four biological replicates; asterisk indicates significant difference compared with control, $p = 0.0078$ (Student's *t*-test). **(F)** *Nicotiana benthamiana* plants at 4 dpi. Bars shown the means ± SEM obtained from five biological replicates; asterisk indicates significant difference compared with control (*t*-test with Welch's correction, $p = 0.0010$). **(G)** *Oryza sativa* plants at 4 dpi. Bars show the means ± SEM obtained from six biological replicates; asterisk indicates significant difference compared with control (*t*-test with Welch's correction, $p = 0.0001$). On the right it is shown that, in the presence of escin, hyphae hyperproliferate in the inoculated rice leaves and cause necrosis, which extend along the spray-inoculated leaves.

Figure 6D for *N. benthamiana*, which resulted in a 7.7-fold increase in the extent of the necrosis generated by the fungi. The enhanced disease susceptibility mediated by triterpenes saponins appears to be the result of a fungal biomass enhancement, which occurs prior to the emergence of the visible necrosis on the inoculated leaves, as exemplified in *N. benthamiana* plants upon escin treatment (Supplemental Figure 9). Therefore, irrespective of the host plant, triterpenoid saponins exert a remarkable effect on growth and virulence enhancement of *B. cinerea*.

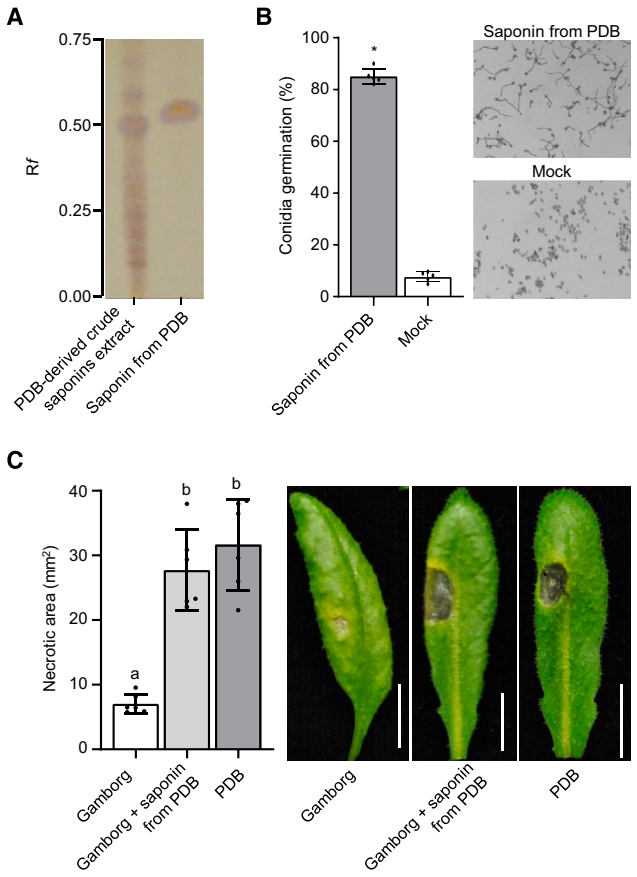

Figure 4. PDB inoculation medium is rich in saponins facilitating *B. cinerea* growth and infection.

(A) Lieberman–Burchard-stained TLC plate reveals the presence of saponins in PDB medium-derived extract. PDB medium was dissolved and processed for saponin identification as described in the section "materials and methods." Left lane, PDB-derived saponin-enriched fraction eluted from a Superdex 75 10/300 column; right lane, sample of the major saponin present in PDB medium purified by preparative TLC.

(B) Conidia germination assay of water-suspended *B. cinerea* spores supplemented with the TLC-purified saponin sample derived from PDB medium (right lane in **A**). Bars show the mean ± SEM obtained from five biological replicates; asterisk indicates significant difference compared with control, $p < 0.0001$ (Student's *t*-test).

(C) Comparative susceptibility of *Arabidopsis* plants to *B. cinerea* infection. *Arabidopsis* plants were inoculated with *B. cinerea* spores (1×10^6 spores/ml) suspended either in Gamborg's B5, Gamborg's B5 supplemented with the TLC-purified PDB-derived saponin (0.1 μg/ml), or Gamborg's B5 supplemented with PDB (6 g/l). Bars represent the mean ± SEM obtained from six biological replicates; different letters among bars indicate significant differences (Brown–Forsythe and Welch ANOVA test; Benjamini, Krieger, and Yekutieli test, $p < 0.01$). A representative leaf from each of the three inoculation media (at 4 dpi) is shown on the right for comparison.

Gamborg B5 vs. potato dextrose broth inoculation medium: Saponins make a difference

B. cinerea is a necrotrophic ascomycete that is commonly cultivated in Petri dishes containing agar supplemented with potato dextrose (PDA) from where conidia are harvested with a 10 mM $MgSO_4$ solution. For infection experiments, the conidial inoculum is routinely supplemented with nutrient-rich medium, particularly when studies involve *Arabidopsis*, a poorly susceptible host for *B. cinerea* (Van Baarlen et al., 2007). However, from a survey of the literature on research performed in *Arabidopsis*, and also based on our own lab experience, we noticed that preparation of conidial inoculum in potato dextrose broth (PDB), rather than in Gamborg B5, renders better infection results. A similar effect on the virulence of *B. cinerea* based on the inoculation medium employed was also observed to occur when inoculations are performed in *E. lathyris* and in *N. benthamiana* (Supplemental Figure 10A and 10B). We hypothesized that the difference between the two media in promoting disease could be based on the presence of saponins in PDB, as this medium derives from potato tubers. To test this hypothesis, we searched for the presence of saponins in PDB. The water-dissolved PDB was extracted with heptane, and the resulting polar phase was recovered and purified using an LC-18 SPE column. The obtained putative saponin-enriched fraction was resolved by TLC and stained with Liebermann–Burchard reagent, which revealed an abundant saponin with an *Rf* value of 0.56 (Figure 4A). The purified saponin obtained from PDB extracts was able to promote germination of water-suspended *B. cinerea* conidia (Figure 4B). Moreover, in comparative inoculation experiments, the supplementation of Gamborg B5 medium with the PDB-isolated saponin rendered a more aggressive infection in *Arabidopsis* than that recorded with Gamborg B5 alone. This infection enhancement due to the addition of the saponin to Gamborg B5 was of a magnitude similar to that recorded for PDB (Figure 4C). Therefore, the effectiveness of the PDB-based inoculum in promoting enhanced virulence of *B. cinerea* leading to more severe necrosis can be explained, at least in in part, by the presence of saponins in PDB.

Escin changes *B. cinerea* growth strategy

To understand the effect of saponins on *B. cinerea* development, we characterized the effects of escin. After 24 h of conidial cultivation, escin promoted a 36% increase in fungal biomass (Figure 5A) due to the differential enlargement of the hyphae (Figure 5B). This growth effect does not appear to be the result of saponin acting as a nutrient, since Gamborg B5 medium is rich in sucrose and its supplementation with an extra dose of sucrose did not mimic the effect of escin (Figure 5B). Interestingly, early monitoring (i.e., 4–8 h) of individualized conidia demonstrated a higher rate of germ tube elongation mediated by escin (Figure 5C). Moreover, analysis of hyphal growth on the leaf surface of *Arabidopsis* plants corroborated the *in vitro* observations, with hyphal growth differences observed at 24 h post infection (hpi) (Supplemental Figure 11). Hyphal enlargement persisted, and the inoculated leaf area became fully covered with intertwined hyphae, which appeared to have developed an epiphytic growth habit with poor penetration into host epidermal cells (Supplemental Figure 11).

Soon after the conidium germination, a swollen chitin-enriched structure differentiates at the apex of the emerging germ tube, corresponding to the single-celled appressorium (Ryder et al., 2022). This appressorium mediates host attachment and early penetration, leading to the release of virulence factors that induce localized host cell damage (Cheung et al., 2020). Interestingly, this early appressorium formation was markedly inhibited by escin (Figure 5D), as observed upon chitin staining with calcofluor (Figure 5D). This appressorium inhibition concurred with sustained elongation of the germ tube.

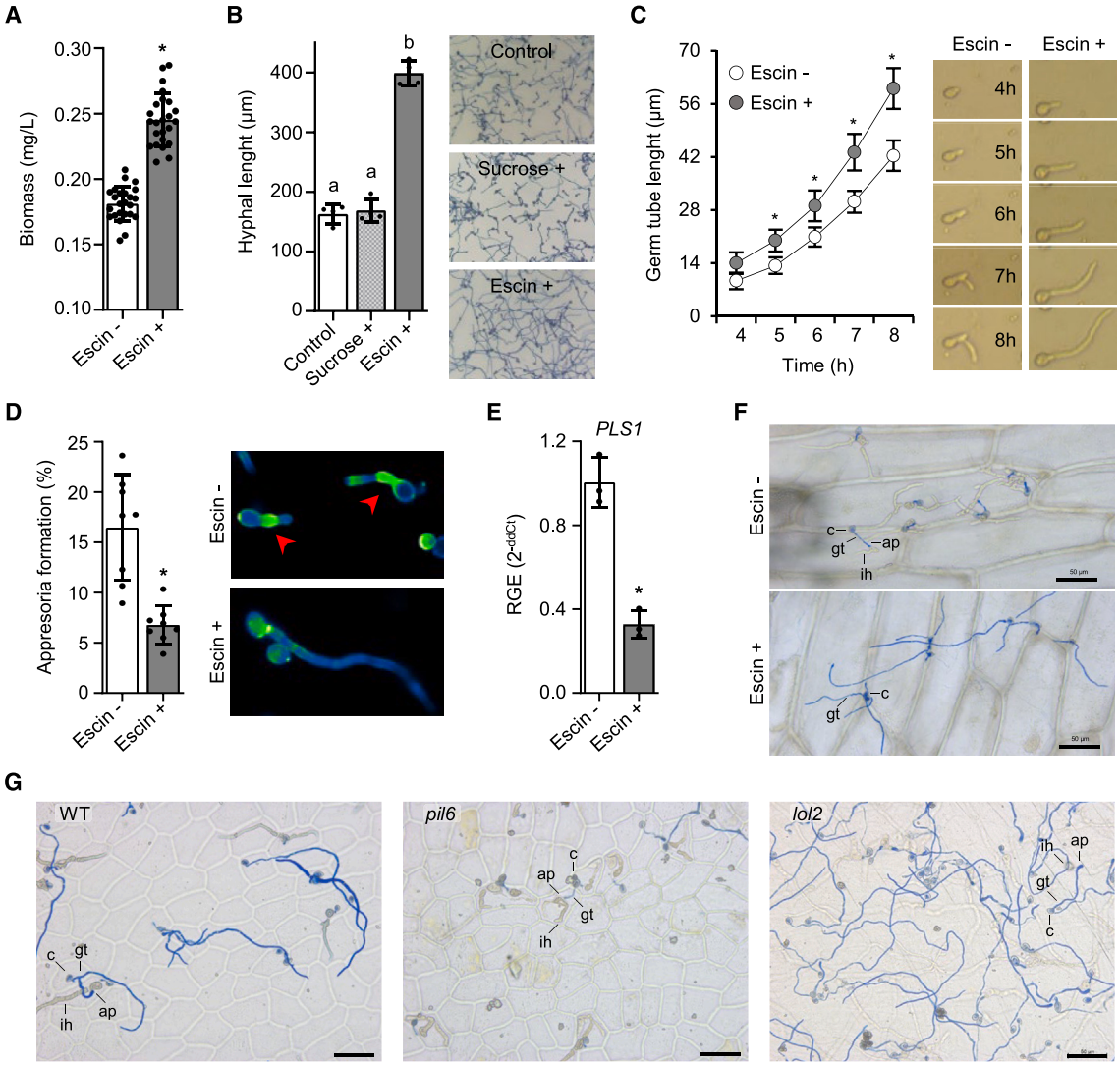

Figure 5. Escin-induced changes in *B. cinerea* growth.

(A) *B. cinerea* biomass accumulated *in vitro* after 24 h of incubation in Gamborg's B5 and Gamborg's B5 supplemented with 0.75 µg escin/ml medium. Bars show the mean ± SEM obtained from 24 biological replicates; asterisk indicates significant difference compared to control, $p < 0.0001$ (*t*-test with Welch's correction).

(B) Hyphal length at 24 h of incubation of conidia in Gamborg's B5 (control), Gamborg's B5 supplemented with sucrose (sucrose+), and Gamborg's B5 supplemented with escin (escin+). Bars show the mean ± SEM obtained from four biological replicates; different letters among bars indicate significant differences ($p < 0.05$; ANOVA test, Bonferroni's test). Pictures on the right show hyphae elongating in the three media.

(C) Time course (from 4 to 8 h) of germ tube elongation in the presence or absence of escin. Points represent the mean ± SEM obtained from eight biological replicates; asterisks indicate significant difference (Student's *t*-test; $p < 0.01$).

(D) Effect of escin on appressoria formation *in vitro* after 8 h of cultivation. Bars represent the mean ± SEM obtained from eight biological replicates; asterisk indicates a significant difference (*t*-test with Welch's correction, $p = 0.0009$). Pictures on the right show calcofluor-derived fluorescence on germinated conidia (from low intensity in blue to high intensity in green). The arrows indicate the presence of appressoria.

(E) Effect of escin on *BcPLS1* expression. Bars show the mean ± SEM obtained from three biological replicates; asterisk indicates a significant difference ($p = 0.0062$; pairwise fixed reallocation randomization test).

(F) Penetration of the onion epidermis by *B. cinerea* at 24 hpi in the absence (escin−) or presence (escin+) of escin. c, conidia; gt, germ tube; ap, appressoria; ih, infective hyphae.

(G) *E. lathyris* leaf epidermal peels from wild-type, *pil6*, and a *lol2* plants at 24 hpi with *B. cinerea*.

Following this observation, we measured the expression of the appressoria-specific marker gene *BcPSL1* (Gourgues et al., 2004), for which we recorded marked repression upon escin treatment (Figure 5E). Appressorium repression is expected to lead to poor early host penetration by the fungi; therefore, we performed comparative see-through fungal penetration assays using onion peels. Figure 5F shows that, upon conidial germination and appressoria formation, the hyphae penetrated the epidermal layer, with initial infection occurring at 24 hpi. Conversely, in the presence of escin, hyphae elongate but do not penetrate the epidermal layer, which results in epiphytic growth on the surface of the onion peel (Figure 5F), a

phenomenon also observed to occur in inoculated *Arabidopsis* leaves (see below) We extended these studies to *E. lathyris* by using leaf epidermal peels. In epidermal peels from wild-type plants, conidia germinated and developed an apparent epiphytic growth habit that concurred with the formation of penetration structures, leading to effective infection by the fungus (Figure 5G). This growth habit ceases to be visible in epidermal peels of the resistant *pil6* plants, which produce no eulasaponins, because conidial germination becomes severely compromised. However, when conidial germination occasionally occurs in *pil6* peels, it takes steps and progresses to form infectious structures. In marked contrast, in leaf epidermal peels of the *lo2* mutant, which produces more triterpenoids (Castelblanque et al., 2018), a much higher proliferation of hyphae takes place that showed an epiphytic growth habit with abundant penetration events taking place (Figure 5G). This might explain why the *lol* mutants showed enhanced disease susceptibility to *B. cinerea* (Figure 2B). Based on these observations, we hypothesized that plant saponins might function as host-derived cues for *B. cinerea* to change its growth strategy and gain infection advantages. Therefore, recognition of plant saponins by *B. cinerea* might represent a strategic evolutionary adaptation of *B. cinerea* for better host colonization.

Escin signals transcriptional reprogramming of *B. cinerea*

To gain insight into the early effects of saponins on *B. cinerea*, we conducted whole-transcriptome comparative expression analysis (RNA sequencing [RNA-seq]) at 18 h of spore cultivation. Differential expression analysis of the RNA-seq data led to the identification of 1088 differentially expressed genes (DEGs; $\geq|2|$ fold change; $p < 0.05$), of which 484 were downregulated and 604 were upregulated by escin (Figure 6A). The validation of this result was tested by qRT-PCR for 24 randomly selected genes showing different fold changes (Supplemental Figure 12A and 12B), which provided a good level of confidence for the RNA-seq data. Among the downregulated genes, 163 encoded for predicted secreted proteins, with 50 of them subclassified as carbohydrate-active enzymes related to host penetration (Lombard et al., 2014), including 24 plant cell wall-degrading enzymes (Glass et al., 2013) (i.e., *BcXyl1*, *BcPg3*, *BcPg4*, or *BcAra1*). Others are related to plant cell degradation, including four cutinases, two proteases (*BcAps6* and *BcAps9*), and sedolisin. In addition, the gene cluster regulating the biosynthesis of the phytotoxin botrydial (i.e., *BcBot1-to-7*), which is important for the virulence of *B. cinerea* (Porquier et al., 2016), elicitors inducing plant cell death (CDIPs; Li et al., 2020) (i.e., *BcNep1*, *Bcleb1*, and *BcChr1*) and *Fascin-like* genes related to virulence and host colonization (i.e., *BcFlp1* and *BcFlp2*), were similarly repressed by escin. Also, of the 54 genes that encode ROS-producing systems (Siegmund and Viefhues, 2016), 13 were downregulated by escin, including aquaporins (i.e., *BcAqp8*, *BcNoxA*, *BcNoxB*, and *BcNoxR*; Segmüller et al., 2008), and ROS scavenging-related genes (*BcPrx5*, *BcCat2*, and *BcSod2*). As ROS play a role in early infection by *B. cinerea* (Govrin and Levine, 2000), their downregulation might indicate that ROS secretion is repressed by escin. Four melanogenic genes (*BcPks13*, *BcScd1*, *BcBrn1*, and *BcBrn2*) key for appressorium formation and host penetration (Schumacher, 2016) were also downregulated by escin, consistent with the inhibition of early appressorium formation. Interestingly, from the 484 downregulated genes, 14 encoded transcription factors (TFs) (Figure 6; Supplemental Table 1). Among them, eight TFs contain the Zn2/Cys6 domain, including the BcZtf1 and BcZtF2 TFs involved in the control of the expression of melanogenic genes mentioned above leading to melanin accumulation (Schumacher, 2016); also, the BcBot6 TF positively regulates the botrydial biosynthetic pathway important for virulence as mentioned above (Porquier et al., 2016) or the BcLtf6 TF involved in light responses (Brandhoff et al., 2017). The homeobox TF BcHox6, a member of the master developmental regulators that play major roles in fungal growth and differentiation (Antal et al., 2012) and two SANT/Myb+Homeodomain TFs, also crucial for light-specific regulation of fungal growth and development (Olivares-Yañez et al., 2021), were similarly downregulated by escin (Supplemental Table 1). In contrast, escin upregulated 124 genes for other predicted secreted proteins, of which 32 were classified as carbohydrate-active enzymes, including 12 related to plant cell wall-degrading enzymes (e.g., BcCel5A, BcXyn10B, BcPg6, and BcPme1), two cutinases, four proteases, and three CDIP elicitors (i.e., BcGs1m, BcNep2, and BcSpl1). Interestingly, members of the RAS-GTPases superfamily, such as *BcRsr1*, which promotes hyphal development (Pulver et al., 2013); the calcineurin pathway, which controls fundamental aspects of growth and development in filamentous fungi (Harren et al., 2012) (e.g., *BcRnr1*, *BcCND3*, or *BcCND8*); and the cyclophilin-dependent gene *BcCpd1*, were upregulated by escin, indicating a growth-promoting activity mediated by escin. Escin also promoted the upregulation of 24 TFs (Supplemental Table 1), including the light-responsive TF BcLtf7, which is involved in promotion of hyphal development and vegetative growth (Schumacher, 2017). Interestingly, nearly half of the escin-mediated upregulated TFs contain the Zn2/Cys6 domain but, for most of them, there is not yet any functional characterization. The Homeobox TF BcHox4, which is required for fungal growth and differentiation (Antal et al., 2012); the BcLtf7 TF mediating light-mediated conidiophore development (Brandhoff et al., 2017); or the TF containing a BZip motif (ID: Bcin02g01550), which is one of the most connected TFs to light-specific gene regulation (Olivares-Yañez et al., 2021), represent other regulators contributing to the orchestration of the transcriptional reprograming of *B. cinerea* mediated by escin. Eulasaponins, but not sucrose, mirrored escin-mediated transcriptional regulation (Supplemental Figure 12B), suggesting that the saponins-mediated effect is not related to nourishment. Taken together, these results indicate that saponins signal a specific transcriptional reprogramming of *B. cinerea*, which represses genes related to the penetration and degradation of plant cell barriers while activating genes controlling vegetative growth and where at least 28 TFs seem to be involved in modulating expression of downstream genes. Further support for saponins functioning as signal molecules comes from the observation that the fluorescent avenacin A-1 saponin is rapidly taken up by the emerging hyphae and shows intracellular accumulation (Supplemental Figure 6C). In fact, *in vitro* kinetic experiments revealed a progressive reduction of the saponin supplemented in the media that inversely correlates with a progressive increase in fungal biomass (Supplemental Figure 13), which suggests *B. cinerea* might be metabolizing saponins. What is responsible for saponin reception, how its internalization is

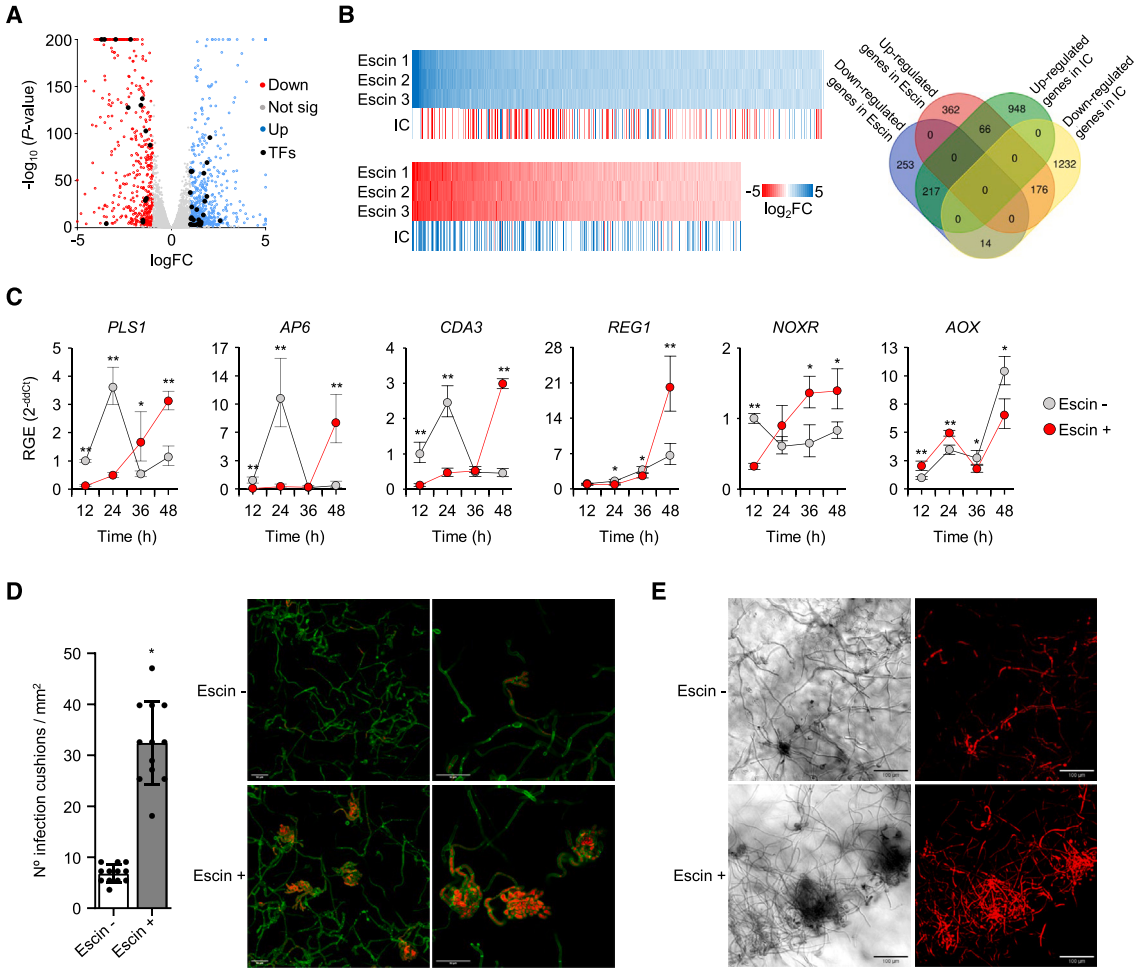

Figure 6. Escin-mediated transcriptional reprogramming of *B. cinerea* and induction of IC structures.

(A) Volcan plot of the transcriptome analysis of *B. cinerea* at 18 h of conidia germination in the absence or presence of escin. Differentially expressed genes (DEGs) with a *p* value ≤0.05 and a log fold change ≤−2 (red point) or ≥2 (blue point) are shown; black points show the DEGs encoding transcription factors (TFs).

(B) Heatmap clustering of up- and downregulated genes (left) and Venn diagram (left) of *B. cinerea* escin-mediated DEGs in comparison with those associated to IC formation (Choquer et al., 2021). The gene number in each case and for each experimental condition is displayed on top of each ellipsoidal circle in the Venn diagram, and common genes are indicated in the intersection of circles, so that the sum of the number within a intersection represents the total number of genes deregulated.

(C) qRT-PCR analysis of selected *B. cinerea* genes at 12, 24, 36, and 48 hpi of *Arabidopsis* plants with conidia suspended in Gamborg's B5 (escin−) or Gamborg's B5 supplemented with escin (escin+). Points show the mean ± SEM obtained from three biological replicates; asterisks indicate significant differences compared with the control (*p <0.05, **p <0.01; pairwise fixed reallocation randomization test).

(D) Formation of ICs in *B. cinerea* after 48 h of *in vitro* incubation in Gamborg's B5 (escin−) or Gamborg's B5 supplemented with escin (escin+). Bars show the mean ± SEM obtained from 12 biological replicates; asterisk indicates a significant difference compared with the control (*t*-test with Welch's correction, $p < 0.0001$). Pictures on the right correspond to confocal images showing calcofluor-derived green fluorescence, which is specific for chitin, in comparison to the eosin Y-derived red fluorescence, which is specific for chitosan.

(E) Confocal images from *A. thaliana* leaves after 48 hpi with *B. cinerea* conidia suspended in Gamborg's B5 (escin−) or Gamborg's B5 supplemented with escin (escin+). The red fluorescence upon eosin Y staining, which is specific for chitosan, revealed the enhanced accumulation of ICs in the presence of escin.

achieved, and what specific signal transduction pathways control the observed transcriptional reprogramming mediated by escin represent a challenge for future research.

Escin leads to hyperproliferation of ICs in *B. cinerea*

If escin signals conidial germination and inhibition of early appressorium formation, how is this mode of action later on transformed into a more aggressive form of the pathogen to cause severe disease? It is important to note that, in addition to the early formation of UAs, which is required for the initial penetration of the plant cell soon after conidia germinate, at later stages of fungal growth and as part of its infection strategy, *B. cinerea* also generates multicellular branched appressoria referred to as IC. At variance to UA formation, IC development takes place at later stages of infection and concurs with enhanced fungal biomass accumulation (Backhouse and Willetts, 1987), where the ICs serve for the massive secretion of fungal destructive

weapons leading to the severe tissue destruction characteristic of fungal necrotrophic pathogens (de Vallée et al., 2019; Choquer et al., 2021). IC formation in *B. cinerea* carries the concurrent upregulation of more than 1000 genes as well as the downregulation of an additional 1500 genes (Choquer et al., 2021). Interestingly, a comparison of the escin-deregulated genes shown above with those associated with IC formation *in vitro* at 44 hpi (Choquer et al., 2021) revealed opposing gene expression patterns. A total of 29.2% of the genes upregulated by escin (176 genes) appeared repressed during IC formation; conversely, 44.8% of the escin-downregulated genes (217 genes) were upregulated in IC (Figure 6B). This reconciles with a mode of action of escin serving to repress an initial penetration strategy during the early stages of infection due to inhibition of UA formation. This inhibition of UA formation allows the hyphae to keep enlarging epiphytically and consequently facilitating the growth expansion of the pathogen on the plant surface (Figure 5), which ultimately leads to fungal biomass enhancement. To gain further insight into this mechanism, we performed a comparative 12- to 48-h time course of gene expression analysis by qRT-PCR in inoculated *Arabidopsis* plants. Some of the genes early repressed by escin *in vitro*, but highly induced during IC formation, were entertained, including *PSL1* (required for appressorium formation; Gourgues et al., 2004; Siegmund et al., 2013), *AP6* (responsible for fungal virulence; Have et al., 2010), *CDA3* (in charge of chitosan production from chitin; Choquer et al., 2021), *REG1* (critical for production of the phytotoxic botrydial sesquiterpene; Michielse et al., 2011), *NOXR* (critical for ROS production; Segmüller et al., 2008), and *AOX* (involved in development, pathogenicity, and oxidative stress response; Lin et al., 2019). These analyses revealed that, in control inoculated plants, there was an early peak in gene expression at 24 hpi, which drastically declined at 36 hpi. This spike in expression was common for *PSL1*, *AP6*, and *CDA3* (Figure 6C). This early transient expression pattern was repressed in the presence of escin, which reconciles with inhibition of early UA formation shown above (Figure 5D–5F). However, this early escin-mediated repression operates only temporarily, since, at later stages of infection (48 hpi), presumably when the applied saponin has been metabolized and the enhanced biomass has taken place, the IC marker genes become strongly activated and reach higher levels of expression than in the inoculated control plants. Furthermore, *REG1*, another IC marker (Choquer et al., 2021), was only abruptly expressed at late stages (48 hpi) in escin-treated plants (Figure 6C). As for *NOXR*, its induction in the saponin-treated plants progressed gradually over time and reached a higher level of expression than that in the control plants. The expression of *AOX* was slightly higher at 12 and 24 hpi in the presence of escin but not at 48 h. We hypothesized that saponins might be sensed as a plant morphogenetic cue by *B. cinerea* to alter its infection strategy by signaling early inhibition of UA formation that thus impeded early plant penetration upon inoculation. This, in turn, results in boosting epiphytic growth in the fungus leading to abundant biomass proliferation that may be prone to developing ICs. If so, one would expect that escin treatment may result in enhancement of IC development at later times, which might not be a direct effect of the saponin but a consequence of the saponin having promoted enhanced fungal biomass. To test this idea, we searched for the presence of IC structures by fluorescence microscopy upon staining with eosin Y, which stains chitosan (a metabolic marker of ICs). As shown in Figure 6D, 48 h after *in vitro* conidial germination, escin provoked a four-fold increase in the abundance of IC structures. These abundant IC structures appeared as multicellular appressoria, which were enlarged and composed of numerous cells with entangled ramifications. In the absence of escin, the ICs formed were low in abundance, consisting of only a few cells, and were barely branched. When searched *in planta* (Figure 4E), escin also promoted abundant formation of ICs, which were enlarged and highly branched, thriving on the leaf surface, to the extent that they could be easily detected even under a light microscope at 48–60 hpi, appearing as entangled cell clumps surrounded by mycelia. In the absence of escin, the *in planta*-developed ICs were low in abundance, small, and poorly branched, consistent with those observed *in vitro*.

It is noteworthy that escin seems not to directly induce IC formation, since refreshing of the incubation medium with a new supply of the saponin maintains the vegetative growth progression while keeping IC formation reduced (Supplemental Figure 14). Moreover, when assayed *in planta*, the hyperproliferation of ICs occurring as a consequence of saponin treatment only takes place at a time when the added saponin becomes drastically reduced by the presence of the growing fungi (Supplemental Figure 15). This suggest that triterpenoid saponins, initially identified as inhibitors of appressoria formation, induce a change in the infection strategy of *B. cinerea* in favor of virulence. Therefore, saponins signal an early and complex transcriptional reprogramming in *B. cinerea* that leads to a change in its growth habit, which at later stages culminates in the enhanced development of ICs, the multicellular appressoria dedicated to plant penetration and necrotrophy. This provides an explanation for how plant saponins function as disease susceptibility (S) factors that promote pathogenicity in *B. cinerea*.

DISCUSSION

In their natural environment, pathogens develop infection strategies that are crucial for virulence and result in disease progression. To counteract intruders, plants produce a large number of secondary metabolites with antimicrobial activities (Ahuja et al., 2012). Some are synthesized following a pathogenic attack (i.e., phytoalexins), while others are preformed (i.e., phytoanticipins). Saponins have long been considered phytoanticipin-type secondary metabolites that are present in a wide range of plant species (Moses et al., 2014). Saponins are amphiphilic glycosylated molecules derived from three different classes of lipophilic secondary metabolites (triterpenoids, steroids, and steroidal alkaloid molecules; Mugford and Osbourn, 2013), which indicate different structure-based mechanisms in their mode of action. Different saponins have long been considered antimicrobial phytoprotectants; however, extensive genetic evidence of their role is lacking. One exception is the study by Papadopoulou et al. (1999), which characterized oat *sad* mutants that were defective in saponins. The genus *Avena* is the only one among the Gramineae that synthesizes saponins, known as avenacins, which accumulate only in the roots (Osbourn et al., 1994; Osbourn, 1996). The *sad* mutants showed compromised resistance to the root fungus

Gaeumannomyces graminis var. *tritici*, which causes the ''take-all'' diseases in cereals. This compromised resistance appeared to be restricted to root fungi, as the same *sad* mutants showed no differences from wild-type plants when leaf-infecting fungi were used (Papadopoulou et al., 1999). Pathogens have developed saponin-detoxifying enzymes (saponinases) to counteract saponins. Avenacinase (Avn) from *G. graminis* var. *avenae* (Bowyer et al., 1995) deglycosylate and detoxify the oat saponin avenacin A-1 and represents a singular determinant of the pathogen's capacity to infect oats, with *Avn*-minus mutants losing oat infection capacity but retaining pathogenicity in the saponin-deficient host, wheat (Bowyer et al., 1995). Similarly, *Septoria lycopersici* and other tomato-infecting fungal pathogens, including *B. cinerea*, utilize a tomatinase enzyme to deglycosylate α-tomatine, a steroidal alkaloid-type saponin, to infect green tomato fruits (Quidde et al., 1998; Roldán-Arjona et al., 1999). Therefore, saponin-saponinase combinations might affect the outcome of the disease (Martin-Hernandez et al., 2000; Bouarab et al., 2002).

In the present study, we identified a new role of plant saponins. Several lines of evidence indicate that triterpenoid saponins act as determinants of host disease susceptibility to *B. cinerea*. Previous observations of the gained resistance to *B. cinerea* in the *E. lathyris* laticifer-deficient *pil1* mutant (Castelblanque et al., 2021) indicated that a compound produced in laticifer cells is important for the pre-penetration phase of the fungi and for disease development. Here, we identified a series of saponins, referred to as eulasaponins, with those carrying lanosterol and butyrospermol triterpene scaffolds being the most conspicuous, which mediate disease susceptibility to *B. cinerea* in *E. lathyris*. These triterpenes, in their free non-conjugated form, accumulate in the laticifer cells of *E. lathyris* (Castelblanque et al., 2016). In plants, triterpenes are derived from 2,3-oxydosqualene by OSCs enzymes, the first committed step in triterpene biosynthesis and, therefore, for the subsequent biosynthesis of saponins (Thimmappa et al., 2014). We identified three laticifer-specific *OSCs* genes, one encoding LAS and two encoding butyrospermol synthases (BUT1 and BUT2). Individual or combined downregulation of these *OSCs* genes in *E. lathyris* using VIGS resulted in resistance enhancement to *B. cinerea*, therefore mirroring laticifer-deficient *pil* mutants, which unveils the importance of maintaining intact triterpene biosynthesis for *B. cinerea* to promote disease in *E. lathyris*. Further insight into the importance of saponins derived from the *M. truncatula lha-1* mutant, in which the biosynthesis of medicagenic and zanhic acid glycosides (the major saponins in the leaves) is blocked (Carelli et al., 2011). In *lha-1* plants, similar to *pil* plants, resistance to *B. cinerea* was remarkably enhanced. Moreover, other plant saponins, such as escin and avenacin-A1, mimic the effect of eulasaponins in promoting disease susceptibility to *B. cinerea*. In fact, chemical complementation of the gained-resistance phenotype of *lha-1* and *pil* mutants by saponins provided further evidence for the role of plant saponins as a host susceptibility (S) factor. Saponin-mediated disease promotion was also observed in different plant species, and particularly interesting were the cases of *N. benthamiana* and rice plants, as there is a lack of gray mold disease reported for them, and neither synthesizes triterpenoid saponins. However, the application of saponins promotes disease development. These observations highlight the significance of the chemical recognition of triterpenoid saponins by *B. cinerea*, and we speculate that they might function as cues to identify the host and initiate fungal development, leading to disease. In general, plant triterpenoids, either in their free or conjugated forms, abundantly accumulate in the cuticular wax of different plant organs, including both the intracuticular layer embedded in the cutin matrix and the epicuticular layer on the outer surface (Van Maarseveen and Jetter, 2009; Buschhaus and Jetter, 2011), which are actively transported from their place of synthesis using still poorly understood mechanisms and that in most cases includes either a vesicle-based transport, a transporter-mediated transport, or a liquid-liquid phase separation (Fang and Xiao, 2021). In the case of *E. lathyris* plants, laticifer cells are the major source of triterpenoids and saponins, and these cells are distributed internally in close contact with the external epidermal layer (Castelblanque et al., 2018). This might favor that the laticifer-synthesized saponins can easily reach the cuticular layers, where they could be easily identified by an attacking pathogen and exert their proposed role as provirulent factors. In fact, the laticifer-free leaf epidermal layer (i.e., epidermal peels) of *E. lathyris* plants, which represents ca. 5% of the total fresh weight (FW) of the entire leaf organ, is rich in saponins (0.79 $\pm$ 0.04 μg equiv escin/mg FW) (Supplemental Figure 16). In their mode of action, saponins promote conidial germination and germ-tube elongation concurrently with the repression of single-celled appressoria (UA) formation, which impedes early host penetration by the fungi and facilitates boosting the spreading of enlarging hyphae that adopt an epiphytic growth habit in the inoculated leaf. This in turn leads to enhanced accumulation of fungal biomass that expands from the initial inoculation point. This change in the growth habit of *B. cinerea* mediated by saponins, which finally results in higher fungal biomass growing epiphytically in the inoculated plant surface, ultimately renders the abundant formation of highly specialized multicellular appressoria, known as ICs. Escin-mediated increased IC formation seems to be an indirect consequence of the saponin action and appears to only obey to the change of the growth strategy of the fungi. The continued presence of saponins in the incubation medium keeps IC formation repressed, thus suggesting that it is only after the signal molecule has been consumed by the hyperproliferating fungi that the gene repression effect on appressorium formation is released and prolific IC structures emerge. Since the IC is considered a fungal structure for efficient plant penetration and plant-biomass destruction (Choquer et al., 2021), its hyperproliferation might explain why *B. cinerea* becomes hypervirulent and generates acute necrosis in the presence of saponins. We propose that saponins function as host cues or morphogens that trigger early transcriptional reprogramming of fungi, with 1088 genes significantly altered at the early stages of saponin perception. Remarkably, 484 genes downregulated at early stages of saponin application appeared to be upregulated during IC formation, whereas most of the 604 upregulated genes were downregulated during IC formation. However, this early saponin-mediated expression pattern occurs only transiently, which might strategically facilitate vegetative proliferation of the fungus and colonization of the host. At a later stage, genes required for penetration and virulence of the fungal necrotroph gain strong expression, which concurs with the abundant proliferation of ICs structures. The massive proliferation of ICs, as the ultimate consequence of the saponins-mediated growth and infection strategy, guarantees the success of *B. cinerea*

over its host. We speculate that, during the course of armrace evolution in natural environments, *B. cinerea* may have developed a host identification and growth adaptation strategy based on the presence of saponins synthesized by the host. Therefore, we propose that saponins are novel S factors for *B. cinerea* infection.

A future challenge is to elucidate the signaling mechanism mediating the action of saponins in *B. cinerea*. Another key area of interest is to determine whether other fungal pathogens use a similar strategy to colonize their hosts. In any case, the development of new crop protection strategies to combat gray mold disease through the manipulation of triterpene biosynthesis may complement approaches that exploit the plant's resistance mechanism induced after infection.

METHODS

Plant material and growth conditions

E. lathyris wild-type plants and *pil* and *lol* mutants used here have been described previously (Castelblanque et al., 2016, 2018). Plants were grown in a growth chamber (19°C–23°C, 85% relative humidity, 120–150 μmol m^{-2} s^{-1} fluorescent illumination, 16-h light photoperiod). Seven-week-old *E. lathyris* plants were used for *B. cinerea* infection assays, and full expanded apical leaves were collected for metabolite analysis. Growth of other plant species was at 19°C–23°C and 16 h of light photoperiod (120–150 μmol m^{-2} s^{-1} fluorescent illumination).

B. cinerea conidial germination and growth measurements

B. cinerea conidia (strain CECT2100, Spanish Type Culture Collection, Universitat de Valencia) were obtained as described by Castelblanque et al. (2021) and germination assays were performed in sterile 96-well ELISA plates (1 × 10^5 conidia/ml) in 10 mM magnesium sulfate. Plates were cultivated for 24 h in dark at 24°C, and the conidial germination ratio was calculated by directly counting germinated and non-germinated conidia under a microscope. Biomass production was determined by spectrometry on a VICTOR X5 Multilabel Plate Reader (PerkinElmer, MA, US) at 450 nm. A reference curve from lyophilized *B. cinerea* hyphae (absorbance = 0.1269 mg/ml + 0.04; R^2 = 0.98) was used to calculate biomass. Hyphal length was recorded using a Diaphot TMD Inverted Microscope (Nikon) and measurements were performed for 40 germinated conidia for each biological repetition (n = 4).

B. cinerea inoculation assays

Plants were inoculated with *B. cinerea* conidia by either spraying at 1 × 10^6 conidia/ml (Castelblanque et al., 2021) or drop application at 1 × 10^5 conidia/ml onto leaves. Conidia were suspended in Gamborg's B5 medium (Duchefa, the Netherlands), supplemented with 10 mM sucrose and 10 mM potassium phosphate at pH 6. When indicated, the conidial suspension was supplemented with 0.75 mg/ml of escin (Sigma-Aldrich). Plants were kept at 100% relative humidity until sampling. Four leaves from at least four plants per treatment were taken, cleared with ethanol, and photographed to evaluate the leaf area affected by necrotic lesions, as described by Castelblanque et al. (2021). Onion and leaf epidermal layer were peeled and strips washed with distilled water and incubated for 1 h at 70°C. A 6-μl droplet of 1 × 10^5 spores of *B. cinerea* was applied and incubated for 24 h in the dark at 24°C and 100% humidity. When indicated, samples were stained with lactophenol-trypan blue (Koch and Slusarenko, 1990) and examined under a light microscope (Leica DM5000).

Microscopy and fungal structures visualization

B. cinerea conidia were cultured in a μ-Slide 8 Well^{high} (Ibidi, Germany) in the dark at 24°C. Confocal images were obtained using a Zeiss AxioObserver 780 confocal microscope (Germany). The fluorescent signal of avenacin was captured using a 405-nm excitation wavelength. For IC visualization, samples were treated with eosin Y and calcofluor as described by Choquer et al. (2021), and confocal imaging was captured at 561- (eosin Y) and 405-nm (Calcofluor) excitation wavelengths. To visualize IC formation *in planta*, confocal microscopy was performed using a Leica Stellaris 8 FALCON confocal microscope (Germany). A Leica DM5000 microscope was used for brightfield images.

Statistical analysis

Homogeneity of variance was evaluated using Levene's test (Levene, 1960) and normal distribution was evaluated using the Shapiro-Wilks test (Shapiro and Wilk, 1965). The number of biological repetitions evaluated and particular statistical parameters are reported in the figures and their legends.

DATA AND CODE AVAILABILITY

The raw sequencing data of *B. cinerea* transcriptome analysis have been deposited in the National Center for Biotechnology Information (NCBI; https://www.ncbi.nlm.nih.gov/). The Sequence Read Archive files can be downloaded from the BioProject PRJNA1021029.

SUPPLEMENTAL INFORMATION

Supplemental information is available at *Molecular Plant Online*.

FUNDING

This research was supported by grants TED2021-130979B-I00 and PID2021-126151OB-I00 to P.V. from the Spanish AEI research agency.

AUTHORS CONTRIBUTIONS

P.V., F.J.E., and A.F.-B. designed the experiments. A.F.-B. performed VIGS experiments. F.J.E. and B.B. carried out microscopy studies. M.P.L.-G. and F.J.E. carried out the HPLC analyses. F.J.E. performed the *B. cinerea* experiments, plant inoculations, and gene expression studies. C.J.A. performed the peelings experiments. P.V. wrote the article.

ACKNOWLEDGMENTS

We thank Javier Forment for assistance in transcriptome analysis, Ana Espinosa for help in GC/MS analysis, José Antonio Darós and Verónica Aragonés for VIGS plasmids and advice, Ornella Calderini for providing the *M. truncatula lha-1* seeds, Lourdes Castelblanque for technical advice, and Victor Flors for reading of the manuscript. No conflict of interest is declared.

Received: November 28, 2023
Revised: February 12, 2024
Accepted: May 27, 2024
Published: May 27, 2024

SUPPORTING CITATIONS

The following references appear in the supplemental information: Anders et al. (2015), Diguta et al. (2010), Dobin et al. (2013), Doyle et al. (1990), Kim et al. (2019), Love et al. (2014), Martin (2011), Pfaffl et al. (2002); Van Kan et al. (2017).

REFERENCES

Abuqamar, S., Ajeb, S., Sham, A., Enan, M.R., and Iratni, R. (2013). A mutation in the expansin-like A2 gene enhances resistance to necrotrophic fungi and hypersensitivity to abiotic stress in *Arabidopsis thaliana*. Mol. Plant Pathol. **14**:813–827.

Ahuja, I., Kissen, R., and Bones, A.M. (2012). Phytoalexins in defense against pathogens. Trends Plant Sci. **17**:73–90.

Anders, S., Pyl, P.T., and Huber, W. (2015). HTSeq-A Python framework to work with high-throughput sequencing data. Bioinformatics **31**:166–169.

Antal, Z., Rascle, C., Cimerman, A., Viaud, M., Billon-Grand, G., Choquer, M., and Bruel, C. (2012). The Homeobox *BcHOX8* gene in *Botrytis cinerea* regulates vegetative growth and morphology. PLoS One **7**:e48134.

Aragonés, V., Aliaga, F., Pasin, F., and Daròs, J.A. (2022). Simplifying plant gene silencing and genome editing logistics by a one-Agrobacterium system for simultaneous delivery of multipartite virus vectors. Biotechnol. J. **17**:2100504.

Backhouse, D., and Willetts, H.J. (1987). Development and structure of infection cushions of *Botrytis cinerea*. Trans. Br. Mycol. Soc. **89**:89–95.

Bednarek, P., Piślewska-Bednarek, M., Svatoš, A., Schneider, B., Doubský, J., Mansurova, M., Humphry, M., Consonni, C., Panstruga, R., Sanchez-Vallet, A., et al. (2009). A glucosinolate metabolism pathway in living plant cells mediates broad-spectrum antifungal defense. Science **323**:101–106.

Bessire, M., Chassot, C., Jacquat, A.C., Humphry, M., Borel, S., Petétot, J.M.C., Métraux, J.P., and Nawrath, C. (2007). A permeable cuticle in Arabidopsis leads to a strong resistance to *Botrytis cinerea*. EMBO J. **26**:2158–2168.

Bi, K., Liang, Y., Mengiste, T., and Sharon, A. (2023). Killing softly: a roadmap of *Botrytis cinerea* pathogenicity. Trends Plant Sci. **28**:211–222.

Bouarab, K., Melton, R., Peart, J., Baulcombe, D., and Osbourn, A. (2002). A saponin-detoxifying enzyme mediates suppression of plant defences. Nature **418**:889–892.

Bowyer, P., Clarke, B.R., Lunness, P., Daniels, M.J., and Osbourn, A.E. (1995). Host range of a plant pathogenic fungus determined by a saponin detoxifying enzyme. Science **267**:371–374.

Brandhoff, B., Simon, A., Dornieden, A., and Schumacher, J. (2017). Regulation of conidiation in *Botrytis cinerea* involves the light-responsive transcriptional regulators BcLTF3 and BcREG1. Curr. Genet. **63**:931–949.

Büschges, R., Hollricher, K., Panstruga, R., Simons, G., Wolter, M., Frijters, A., van Daelen, R., van der Lee, T., Diergaarde, P., Groenendijk, J., et al. (1997). The barley Mlo gene: a novel control element of plant pathogen resistance. Cell **88**:695–705.

Buschhaus, C., and Jetter, R. (2011). Composition differences between epicuticular and intracuticular wax substructures: How do plants seal their epidermal surfaces? J. Exp. Bot. **62**:841–853.

Cantu, D., Vicente, A.R., Labavitch, J.M., Bennett, A.B., and Powell, A.L.T. (2008). Strangers in the matrix: plant cell walls and pathogen susceptibility. Trends Plant Sci. **13**:610–617.

Carelli, M., Biazzi, E., Panara, F., Tava, A., Scaramelli, L., Porceddu, A., Graham, N., Odoardi, M., Piano, E., Arcioni, S., et al. (2011). *Medicago truncatula* CYP716A12 is a multifunctional oxidase involved in the biosynthesis of hemolytic saponins. Plant Cell **23**:3070–3081.

Castelblanque, L., Balaguer, B., Martí, C., Rodríguez, J.J., Orozco, M., and Vera, P. (2016). Novel insights into the organization of laticifer cells: A cell comprising a unified whole system. Plant Physiol. **172**:1032–1044.

Castelblanque, L., Balaguer, B., Marti, C., Orozco, M., and Vera, P. (2018). *LOL2* and *LOL5* loci control latex production by laticifer cells in *Euphorbia lathyris*. New Phytol. **219**:1467–1479.

Castelblanque, L., García-Andrade, J., Martínez-Arias, C., Rodríguez, J.J., Escaray, F.J., Aguilar-Fenollosa, E., Jaques, J.A., and Vera, P. (2021). Opposing roles of plant laticifer cells in the resistance to insect herbivores and fungal pathogens. Plant Commun. **2**:100112.

Cheung, N., Tian, L., Liu, X., and Li, X. (2020). The destructive fungal pathogen *Botrytis cinerea* - insights from genes studied with mutant analysis. Pathogens **9**:923–946.

Choquer, M., Rascle, C., Gonçalves, I.R., De Vallée, A., Ribot, C., Loisel, E., Smilevski, P., Ferria, J., Savadogo, M., Souibgui, E., et al. (2021). The infection cushion of *Botrytis cinerea*: a fungal "weapon" of plant-biomass destruction. Environ. Microbiol. **23**:2293–2314.

Coego, A., Ramirez, V., Gil, M.J., Flors, V., Mauch-Mani, B., and Vera, P. (2005). An arabidopsis homeodomain transcription factor, overexpressor of cationic peroxidase 3, mediates resistance to infection by necrotrophic pathogens. Plant Cell **17**:2123–2137.

Corwin, J.A., and Kliebenstein, D.J. (2017). Quantitative resistance: more than just perception of a pathogen. Plant Cell **29**:655–665.

Costantini, A. (1999). Escin in pharmaceutical oral dosage forms: quantitative densitometric HPTLC determination. Il Farmaco **54**:728–732.

Crombie, L., Mary, W., Crombie, L., and Whiting, D.A. (1984). Isolation of avenacins A-1, A-2, B-1, and B-2 from oat roots: structures of their "aglycones". the avenestergenins. *J. Chem. Soc., Chem. Commun.*. Advance Access published 1984.

de Vallée, A., Bally, P., Bruel, C., Chandat, L., Choquer, M., Dieryckx, C., Dupuy, J.W., Kaiser, S., Latorse, M.P., Loisel, E., et al. (2019). A similar secretome disturbance as a hallmark of non-pathogenic *Botrytis cinerea* ATMT-mutants? Front. Microbiol. **10**.

Dean, R., Van Kan, J.A.L., Pretorius, Z.A., Hammond-Kosack, K.E., Di Pietro, A., Spanu, P.D., Rudd, J.J., Dickman, M., Kahmann, R., Ellis, J., and Foster, G.D. (2012). The Top 10 fungal pathogens in molecular plant pathology. Mol. Plant Pathol. **13**:414–430.

Diguta, C.F., Rousseaux, S., Weidmann, S., Bretin, N., Vincent, B., Guilloux-Benatier, M., and Alexandre, H. (2010). Development of a qPCR assay for specific quantification of *Botrytis cinerea* on grapes. FEMS Microbiol. Lett. **313**:81–87.

Dobin, A., Davis, C.A., Schlesinger, F., Drenkow, J., Zaleski, C., Jha, S., Batut, P., Chaisson, M., and Gingeras, T.R. (2013). STAR: Ultrafast universal RNA-seq aligner. Bioinformatics **29**:15–21.

Doyle, J.J., Doyle, J.L., Doyle, J.A., and Doyle, J. (1990). A rapid total DNA preparation procedure for fresh plant tissue. Focus **12**:13–15.

Ellis, C., Karafyllidis, I., Wasternack, C., and Turner, J.G. (2002). The Arabidopsis mutant cev1 links cell wall signaling to jasmonate and ethylene responses. Plant Cell **14**:1557–1566.

Fang, Y., and Xiao, H. (2021). The transport of triterpenoids. Biotechnology Notes **2**:11–17.

Fillinger, S., and Elad, Y. (2015). Botrytis - the Fungus, the Pathogen and its Management in Agricultural Systems (Springer International Publishing).

García-Andrade, J., Ramírez, V., López, A., and Vera, P. (2013). Mediated plastid RNA editing in plant immunity. PLoS Pathog. **9**:e1003713.

García-Andrade, J., González, B., Gonzalez-Guzman, M., Rodriguez, P.L., and Vera, P. (2020). The role of aba in plant immunity is mediated through the pyr1 receptor. Int. J. Mol. Sci. **21**:1–22.

Glass, N.L., Schmoll, M., Cate, J.H.D., and Coradetti, S. (2013). Plant cell wall deconstruction by ascomycete fungi. Annu. Rev. Microbiol. **67**:477–498.

Góral, I., and Wojciechowski, K. (2020). Surface activity and foaming properties of saponin-rich plants extracts. Adv. Colloid Interface Sci. **279**.

Gourgues, M., Brunet-Simon, A., Lebrun, M.H., and Levis, C. (2004). The tetraspanin BcPls1 is required for appressorium-mediated

penetration of *Botrytis cinerea* into host plant leaves. Mol. Microbiol. **51**:619–629.

Govrin, E.M., and Levine, A. (2000). The hypersensitive response facilitates plant infection by the necrotrophic pathogen *Botrytis cinerea*. Curr. Biol. **10**:751–757.

Harren, K., Schumacher, J., and Tudzynski, B. (2012). The Ca2+/calcineurin-dependent signaling pathway in the gray mold botrytis cinerea: the role of calcipressin in modulating calcineurin activity. PLoS One **7**:e41761.

ten Have, A., Espino, J.J., Dekkers, E., Van Sluyter, S.C., Brito, N., Kay, J., González, C., and van Kan, J.A.L. (2010). The *Botrytis cinerea* aspartic proteinase family. Fungal Genet. Biol. **47**:53–65.

Humphry, M., Consonni, C., and Panstruga, R. (2006). mlo-based powdery mildew immunity: silver bullet or simply non-host resistance? Mol. Plant Pathol. **7**:605–610.

Kim, D., Paggi, J.M., Park, C., Bennett, C., and Salzberg, S.L. (2019). Graph-based genome alignment and genotyping with HISAT2 and HISAT-genotype. Nat. Biotechnol. **37**:907–915.

Koch, E., and Slusarenko, A. (1990). Arabidopsis is susceptible to infection by a downy mildew fungus. Plant Cell **2**:437–445.

Laluk, K., Luo, H., Chai, M., Dhawan, R., Lai, Z., and Mengiste, T. (2011). Biochemical and genetic requirements for function of the immune response regulator BOTRYTIS-INDUCED KINASE1 in plant growth, ethylene signaling, and PAMP-triggered immunity in Arabidopsis. Plant Cell **23**:2831–2849.

Levene, H. (1960). Robust test for equality of variances. In Contributions to Probability and Statistics: Essays in Honor of Harold Hotelling, I. Olkin and H. Hotelling, eds. (Stanford University Press), pp. 278–292.

Li, Y., Han, Y., Qu, M., Chen, J., Chen, X., Geng, X., Wang, Z., and Chen, S. (2020). Apoplastic cell death-inducing proteins of filamentous plant pathogens: roles in plant-pathogen interactions. Front. Genet. **11**:e661.

Lin, Z., Wu, J., Jamieson, P.A., and Zhang, C. (2019). Alternative oxidase is involved in the pathogenicity, development, and oxygen stress response of *Botrytis cinerea*. Phytopathology **109**:1679–1688.

Lombard, V., Golaconda Ramulu, H., Drula, E., Coutinho, P.M., and Henrissat, B. (2014). The carbohydrate-active enzymes database (CAZy) in 2013. Nucleic Acids Res. **42**:490–495.

López, A., Ramírez, V., García-Andrade, J., Flors, V., and Vera, P. (2011). The RNA silencing enzyme RNA polymerase V is required for plant immunity. PLoS Genet. **7**:e1002434.

Lorenzo, O., Chico, J.M., Sánchez-Serrano, J.J., and Solano, R. (2004). *JASMONATE-INSENSITIVE1* encodes a MYC transcription factor essential to discriminate between different jasmonate-regulated defense responses in arabidopsis. Plant Cell **16**:1938–1950.

Love, M.I., Huber, W., and Anders, S. (2014). Moderated estimation of fold change and dispersion for RNA-seq data with DESeq2. Genome Biol. **15**:550.

Martin, M. (2011). Cutadapt removes adapter sequences from high-throughput sequencing reads. EMBnet. j. **17**:10–12.

Martin-Hernandez, A.M., Dufresne, M., Hugouvieux, V., Melton, R., and Osbourn, A. (2000). Effects of targeted replacement of the tomatinase gene on the interaction of Septoria lycopersici with tomato plants. Mol. Plant Microbe Interact. **13**:1301–1311.

Mengiste, T. (2012). Plant immunity to necrotrophs. Annu. Rev. Phytopathol. **50**:267–294.

Michielse, C.B., Becker, M., Heller, J., Moraga, J., Collado, I.G., and Tudzynski, P. (2011). The *Botrytis cinerea* Reg1 protein, a putative transcriptional regulator, is required for pathogenicity, conidiogenesis, and the production of secondary metabolites. Mol. Plant Microbe Interact. **24**:1074–1085.

Moses, T., Papadopoulou, K.K., and Osbourn, A. (2014). Metabolic and functional diversity of saponins, biosynthetic intermediates and semi-synthetic derivatives. Crit. Rev. Biochem. Mol. Biol. **49**:439–462.

Mugford, S.T., and Osbourn, A. (2013). Saponin synthesis and function. In Isoprenoid Synthesis in Plants and Microorganisms: New Concepts and Experimental Approaches (Springer), pp. 405–424.

Olivares-Yañez, C., Sánchez, E., Pérez-Lara, G., Seguel, A., Camejo, P.Y., Larrondo, L.F., Vidal, E.A., and Canessa, P. (2021). A comprehensive transcription factor and DNA-binding motif resource for the construction of gene regulatory networks in *Botrytis cinerea* and *Trichoderma atroviride*. Comput. Struct. Biotechnol. J. **19**:6212–6228.

Osbourn, A.E. (1996). Preformed antimicrobial compounds and plant defense against fungal attack. Plant Cell **8**:1821–1831.

Osbourn, A.E. (2003). Saponins in cereals. Phytochemistry **62**:1–4.

Osbourn, A.E., Clarke, B.R., Lunness, P., Scott, P., and Daniels, M.J. (1994). An oat species lacking avenacin is susceptible to infection by *Gaeumannomyces graminis* var. *tritici*. Physiol. Mol. Plant Pathol. **45**:457–467.

Papadopoulou, K., Melton, R.E., Leggett, M., Daniels, M.J., and Osbourn, A.E. (1999). Compromised disease resistance in saponin-deficient plants. Proc. Natl. Acad. Sci. USA **96**:12923–12928.

Pfaffl, M.W., Horgan, G.W., and Dempfle, L. (2002). Relative expression software tool (REST©) for group-wise comparison and statistical analysis of relative expression results in real-time PCR. Nucleic Acids Res. **30**:e36.

Poinssot, B., Vandelle, E., Bentéjac, M., Adrian, M., Levis, C., Brygoo, Y., Garin, J., Sicilia, F., Coutos-Thévenot, P., and Pugin, A. (2003). The Endopolygalacturonase 1 from *Botrytis cinerea* activates grapevine defense reactions unrelated to its enzymatic activity. MPMI (Mol. Plant-Microbe Interact.) **16**:553–564.

Porquier, A., Morgant, G., Moraga, J., Dalmais, B., Luyten, I., Simon, A., Pradier, J.M., Amselem, J., Collado, I.G., and Viaud, M. (2016). The botrydial biosynthetic gene cluster of *Botrytis cinerea* displays a bipartite genomic structure and is positively regulated by the putative Zn(II)2Cys6 transcription factor BcBot6. Fungal Genet. Biol. **96**:33–46.

Pulver, R., Heisel, T., Gonia, S., Robins, R., Norton, J., Haynes, P., and Gale, C.A. (2013). Rsr1 focuses CDC42 activity at hyphal tips and promotes maintenance of hyphal development in *Candida albicans*. Eukaryot. Cell **12**:482–495.

Quidde, T., Osbourn, A.E., and Tudzynski, P. (1998). Detoxification of alpha-tomatine by *Botrytis cinerea*. Physiol. Mol. Plant Pathol. **52**:151–165.

Ramírez, V., Agorio, A., Coego, A., García-Andrade, J., Hernández, M.J., Balaguer, B., Ouwerkerk, P.B.F., Zarra, I., and Vera, P. (2011). MYB46 modulates disease susceptibility to *Botrytis cinerea* in Arabidopsis. Plant Physiol. **155**:1920–1935.

Ramírez, V., García-Andrade, J., and Vera, P. (2011). Enhanced disease resistance to *Botrytis cinerea* in myb46 Arabidopsis plants is associated to an early downregulation of CesA genes. Plant Signal. Behav. **6**:911–913.

Rohmer, M. (1999). The mevalonate-independent methylerythritol 4-phosphate (MEP) pathway for isoprenoid biosynthesis, including carotenoids. Pure Appl. Chem. **71**:2279–2284.

Roldán-Arjona, T., Pérez-Espinosa, A., and Ruiz-Rubio, M. (1999). Tomatinase from *Fusarium oxysporum* f. sp. *lycopersici* defines a new class of saponinases. Mol. Plant Microbe Interact. **12**:852–861.

Ryder, L.S., Cruz-Mireles, N., Molinari, C., Eisermann, I., Eseola, A.B., and Talbot, N.J. (2022). The appressorium at a glance. J. Cell Sci. **135**:jcs259857.

Sawai, S., and Saito, K. (2011). Triterpenoid biosynthesis and engineering in plants. Front. Plant Sci. **2**:25.

Schumacher, J. (2016). DHN melanin biosynthesis in the plant pathogenic fungus *Botrytis cinerea* is based on two developmentally regulated key enzyme (PKS)-encoding genes. Mol. Microbiol. **99**:729–748.

Schumacher, J. (2017). How light affects the life of *Botrytis*. Fungal Genet. Biol. **106**:26–41.

Segmüller, N., Kokkelink, L., Giesbert, S., Odinius, D., Van Kan, J., and Tudzynski, P. (2008). NADPH oxidases are involved in differentiation and pathogenicity in *Botrytis cinerea*. Mol. Plant Microbe Interact. **21**:808–819.

Senthil-Kumar, M., and Mysore, K.S. (2014). Tobacco rattle virus-based virus-induced gene silencing in *Nicotiana benthamiana*. Nat. Protoc. **9**:1549–1562.

Shapiro, S.S., and Wilk, M.B. (1965). An analysis of variance test for normality (complete samples). Biometrika **52**:591–611.

Siegmund, U., and Viefhues, A. (2016). Reactive Oxygen Species in the Botrytis – Host Interaction. In Botrytis – the Fungus, the Pathogen and its Management in Agricultural Systems, S. Fillinger and Y. Elad, eds. (Springer International Publishing), pp. 269–289.

Siegmund, U., Heller, J., van Kan, J.A.L., and Tudzynski, P. (2013). The NADPH oxidase complexes in *Botrytis cinerea*: evidence for a close association with the ER and the tetraspanin Pls1. PLoS One **8**:e55879.

Smith, C.A., O'Maille, G., Want, E.J., Qin, C., Trauger, S.A., Brandon, T.R., Custodio, D.E., Abagyan, R., and Siuzdak, G. (2005). METLIN: A Metabolite Mass Spectral Database. Ther. Drug Monit. **27**:747–751.

Stochmal, A., Oleszek, W., and Kapusta, I. (2008). TLC of triterpenes (including saponins). In Thin Layer Chromatography in Phytochemistry, pp. 519–541.

Tava, A., and Avato, P. (2006). Chemical and biological activity of triterpene saponins from *Medicago* species. Nat. Prod. Commun. **1**:1180.

Thimmappa, R., Geisler, K., Louveau, T., O'Maille, P., and Osbourn, A. (2014). Triterpene biosynthesis in plants. Annu. Rev. Plant Biol. **65**:225–257.

Van Atta, G.R., and Guggolz, J. (1958). Forage Constituents, Detection of Saponins and Sapogenins on Paper Chromatograms by Liebermann-Burchard Reagent. J. Agric. Food Chem. **6**:849–850.

Van Baarlen, P., Woltering, E.J., Staats, M., and Van Kan, J.A.L. (2007). Histochemical and genetic analysis of host and non-host interactions of Arabidopsis with three *Botrytis species*: An important role for cell death control. Mol. Plant Pathol. **8**:41–54.

Van Kan, J.A.L. (2006). Licensed to kill: the lifestyle of a necrotrophic plant pathogen. Trends Plant Sci. **11**:247–253.

Van Kan, J.A.L., Stassen, J.H.M., Mosbach, A., Van Der Lee, T.A.J., Faino, L., Farmer, A.D., Papasotiriou, D.G., Zhou, S., Seidl, M.F., Cottam, E., et al. (2017). A gapless genome sequence of the fungus *Botrytis cinerea*. Mol. Plant Pathol. **18**:75–89.

Van Maarseveen, C., and Jetter, R. (2009). Composition of the epicuticular and intracuticular wax layers on *Kalanchoe daigremontiana* (Hamet et Perr. de la Bathie) leaves. Phytochemistry **70**:899–906.

Van Schie, C.C.N., and Takken, F.L.W. (2014). Susceptibility genes 101: How to be a good host. Annu. Rev. Phytopathol. **52**:551–581.

Veronese, P., Nakagami, H., Bluhm, B., AbuQamar, S., Chen, X., Salmeron, J., Dietrich, R.A., Hirt, H., and Mengiste, T. (2006). The membrane-anchored BOTRYTIS-INDUCED KINASE1 plays distinct roles in Arabidopsis resistance to necrotrophic and biotrophic pathogens. Plant Cell **18**:257–273.

Wang, Y., Li, X., Fan, B., Zhu, C., and Chen, Z. (2021). Regulation and function of defense-related callose deposition in plants. Int. J. Mol. Sci. **22**:2393–2415.

Wang, M., Gu, Z., Fu, Z., and Jiang, D. (2021). High-quality genome assembly of an important biodiesel plant. *Euphorbia lathyris* L. *DNA Research* **28**.

Yuan, M., Ngou, B.P.M., Ding, P., and Xin, X.F. (2021). PTI-ETI crosstalk: an integrative view of plant immunity. Curr. Opin. Plant Biol. **62**:102030.